Bachelor's thesis

NTNU
Norwegian University of Science and Technology
Faculty of Engineering
Department of Energy and Process Engineering

Ole-Herman Bergem
Håkon Runde
Preben Trana Storsveen

Comparative Weibull Analysis for Estimating Wind Farm AEP with PyWake

Bachelor's thesis in Engineering, Renewable Energy
Supervisor: Tania K. Bracchi
Co-supervisor: David Hulme, Charlotte Obhrai
May 2024

NTNU
Norwegian University of
Science and Technology

Ole-Herman Bergem
Håkon Runde
Preben Trana Storsveen

Comparative Weibull Analysis for Estimating Wind Farm AEP with PyWake

Bachelor's thesis in Engineering, Renewable Energy
Supervisor: Tania K. Bracchi
Co-supervisor: David Hulme, Charlotte Obhrai
May 2024

Norwegian University of Science and Technology
Faculty of Engineering
Department of Energy and Process Engineering

NTNU
Norwegian University of
Science and Technology

Oppgavens tittel: Sammenlikning av Weibull Analyse for å Estimere Vindpark AEP med Pywake **Project title (ENG):** Comparative Weibull Analysis for Estimating Wind Farm AEP with PyWake	**Gitt dato:** 11.01.2024 **Innleveringsdato:** 22.05.2024 **Antall sider rapport / sider vedlagt:** 62 / 9
Gruppedeltakere: Ole-Herman Bergem (10010) olehermb@stud.ntnu.no Håkon Runde (10049) haakorun@stud.ntnu.no Preben Trana Storsveen (10037) prebents@stud.ntnu.no	**Prosjektnummer:** BIFOREN24 1 **Veileder:** Tania K. Bracchi

Fritt tilgjengelig: ☐

Tilgjengelig etter avtale med oppdragsgiver: ☒

Rapporten frigitt etter:

Gruppedeltakernes signatur:

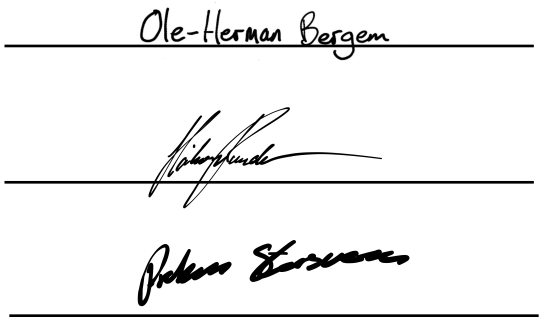

Contents

List of Figures iv

List of Tables v

Preface vi

Abstract vii

Sammendrag viii

List of Abbreviation ix

List of Symbols x

1 Introduction 1

2 Theory 2

2.1 Wakes and PyWake . . . 2

2.2 Annual Energy Production . . . 6

2.3 Wind direction and wind speed . . . 6

2.4 Site Object . . . 8

2.5 Weibull distribution . . . 8

2.6 Kolmogorov-Smirnov test . . . 11

3 Method and Materials 12

3.1 Wind and production data . . . 12

3.2 Dudgeon . . . 13

3.3 Anholt . . . 14

3.4 Power curve and thrust coefficient . . . 15

3.5 Simulations . . . 15

3.6 KS test . . . 20

3.7 Wind sector analysis . . . 20

3.8 Source of error and assumptions . . . 21

4 Results 22

4.1 Weibull fit to wind data at Dudgeon . . . 22
4.2 Dudgeon vs Anholt . . . 26
4.3 Combination of MLE and L-BFGS-B at Dudgeon . . . 29
4.4 AEP results . . . 30

5 Discussion **32**
5.1 Wind data analysis . . . 32
5.2 AEP analysis . . . 33
5.3 Time Series Evaluation . . . 35
5.4 Further work . . . 36

6 Conclusion **37**

Bibliography **i**

Appendix **vi**
A Appendix - Anholt Layout . . . vi
B Appendix - Wind sectors at Dudgeon and Anholt with MLE method . . . vii
C Appendix - Wind sectors at Dudgeon and Anholt with L-BFGS-B method . viii
D Appendix - Weibull parameters for Dudgeon and Anholt with MLE and L-BFGS-B method . . . ix
E Appendix - KS-stat and p-values for Dudgeon and Anholt . . . x
F Appendix - Wind sectors at Dudgeon with MLE method . . . xi
G Appendix - Wind sectors at Dudgeon with L-BFGS-B method . . . xii
H Appendix - Wind sectors for Dudgeon and Anholt with MLE method . . . xiii
I Appendix - Wind sectors for Dudgeon and Anholt with L-BFGS-B method xiv

List of Figures

2.1 Schematic of wake. [6] 2

2.2 Wakes in Horns Rev 1 wind farm, Denmark. [8] 3

2.3 Vertical profiles of mean velocity (top) and velocity (bottom) downstream; top hat. [7] 4

2.4 Gaussian distribution for the velocity deficit in the wake. [7] 4

2.5 Wake expansion. [12] 5

2.6 Example of wind rose layout. [21] 7

2.7 Example of histogram. [23] 7

2.8 Weibull distribution - different values of k. 8

2.9 Weibull distribution - different values of a. 8

2.10 Example of KS-test. [46] 11

3.1 Geographical map, Dudgeon. [50] 13

3.2 Layout of Dudgeon, England. 13

3.3 Geographical map, Anholt. [58] 14

3.4 Layout of Anholt. [48] 14

3.5 Histogram, frequency of wind speed, Dudgeon. 16

3.6 Wind roses, Dudgeon and Anholt for different time periods. 17

3.7 Weibull fitting with MLE and L-BFGS-B for each wind sector at Dudgeon 2019-2020. 18

3.8 KDE wind direction - Dudgeon 2019-2020. 19

4.1 Weibull distribution for Dudgeon - MLE. 22

4.2 Weibull distribution for Dudgeon - L-BFGS-B. 23

4.3 Sector 2, 6, 9 and 11 with MLE for different time intervals at Dudgeon. . . 24

4.4 Sector 0, 1, 3 and 8 with L-BFGS-B for different time intervals at Dudgeon. 25

4.5 Weibull distribution for Dudgeon and Anholt, one-year - MLE. 26

4.6 Weibull distribution for Dudgeon and Anholt, one-year - L-BFGS-B. 28

List of Tables

3.1 Production data and wind data, Dudgeon 12

3.2 Production data and wind data, Anholt 12

3.3 Detailed site information for the Dudgeon wind farm [49, 51, 54, 55, 56] . . 13

3.4 Detailed site information for the Anholt wind farm [57] 14

3.5 Comparison of power curve and C_T values for Dudgeon and Anholt 15

3.6 Data Comparison Across Different Methods and Time Periods 18

3.7 KDE values compared to wind sector AEP amount. 19

3.8 Sample Sizes across Different Sectors 20

4.1 MLE statistics for Dudgeon (one-, 10-, and 20 years) 22

4.2 L-BFGS-B statistics for Dudgeon (one-, 10-, and 20 years) 23

4.3 MLE method KS-stat and p-values for Dudgeon at one-, 10-, and 20 years . 24

4.4 L-BFGS-B method KS-stat and P-values for Dudgeon at one-, 10-, and 20 years 25

4.5 MLE Statistics for Anholt and Dudgeon (one-year) 26

4.6 MLE method KS-stat and P-value for Dudgeon and Anholt, one-year 27

4.7 L-BFGS-B Statistics for Anholt and Dudgeon (one-year) 28

4.8 L-BFGS-B method KS-stat and P-values for Dudgeon and Anholt, one-year 28

4.9 Results of combining MLE and L-BFGS-B methods 29

4.10 AEP with one-year data sample compared to unfiltered production data for Dudgeon 2019-2020 30

4.11 AEP for each sector Dudgeon 2019-2020 with one-year data sample 30

4.12 AEP compared to unfiltered production data for 20-year data sample in Dudgeon 31

4.13 Comparison against AEP 20-year - Dudgeon 31

Preface

This bachelor thesis is the final assignment at the study program Bachelor in renewable energy at Norwegian University of Science and Technology (NTNU) in Trondheim. The group members consist of three students with specialization within wind- and hydro power and effective use of energy.

The project is part of the "Bacheloroppgave Fornybar energi" under the course code of FENT2900. The report along with several other mandatory submissions consists of 100 % of the grade.

The goal of this project is to investigate whether how accurately the Weibull distribution represents the time history of wind data to calculate the annual energy production of offshore wind farms.

The group would like to thank our supervisor Tania Kalogiannidis Bracchi at NTNU for being of great help with feedback and partaking in insightful discussions throughout the project. Also a thank you to our external supervisors from Equinor; David Hulme, Charlotte Obhrai and Nils Joseph Gaukroger, who have provided valuable insight to the topic of offshore wind farms, and technical assistance.

Trondheim 21.05.2024

Ole-Herman Bergem

Abstract

The offshore wind farm sector is expanding, and as such, there is a need for reliable analytical models to profit realize the energy production. This report will use the Python expansion module PyWake, to simulate and assess the annual energy production (AEP) for Dudgeon wind farm from a one-, 10- and 20-year data sample. Results are compared against actual production data from the year 2019-2020, obtained from Equinor. The wind condition parameters for Dudgeon have been sourced from the open source database Nora10. Anholt wind farm is used as a test case to compare findings from the simulations. The study will explore the validity of using Weibull probability density functions as a representation for wind speed dispersion in PyWake's Bastankhah Porté-Agel simulation model, by analyzing the deviation in AEP. Moreover, the Maximum Likelihood Estimation (MLE) and the Limited memory Broyden-Fletcher-Goldfarb-Shanno-Bounds (L-BFGS-B) optimization algorithms will be applied to make the Weibull regressions to facilitate comparisons between different regression tools.

The PyWake module offers a range of scenario based model combinations, that can be defined to the user specific application. The module consist of three main objects, being the site, turbine and wake model object. The wind farm model used in this report is a combination of the uniform Weibull site model and the Bastankhah Porté-Agel wake deficit model, with the turbine and site parameters being specified to the Dudgeon and Anholt cases. The wake deficit model is applicable for far wake scenarios only, therefore disregarding the influence of turbulence intensity and uses a constant wake expansion factor. The site object employs the uniform Weibull model to simulate AEP in conjunction with the wake model. It utilizes twelve Weibull probability functions corresponding to 30°wind direction sectors, each defined by specific shape and scale parameters. The site object also requires a probability of occurrence for each wind sector, which is computed through a kernel density estimation (KDE). The goodness-of-fit for the Weibull regression is assessed using the Kolmogorov–Smirnov test. The results are interpreted based on the KS-stat and p-value, and in relation to the AEP outcomes.

The simulation results reveal that the size of the data sample significantly affects the accuracy of the simulation. Using a one-year data sample, the L-BFGS-B method yielded the most accurate results, with a deviation of only 1.47 % from the actual AEP data. In contrast, with a 20-year data sample, the MLE method showed a smaller deviation of 0.8367 %. The Kolmogorov-Smirnov (KS) test results showed that larger samples produced a lower KS statistic, indicating a closer resemblance to the actual wind speed distribution histogram. Conversely, smaller samples resulted in a statistical resemblance where the p-value exceeded 0.05, suggesting an acceptable fit under the significance level used. Additionally, the AEP for each wind direction sector was analyzed individually. The results indicated varying deviations for all scenarios, and showed to have a correlation with the KDE regression.

This study clearly shows that using the MLE method with larger data samples is preferable for obtaining reliable Annual Energy Production predictions. However, for one-year data samples, the L-BFGS-B method outperforms the alternatives. Further analysis also revealed that Kernel Density Estimation is not a precise method for dividing the probability of occurrence across wind directions. The regression results suggest that KDE does not provide an accurate indication of sector-specific AEP. To enhance the study's reliability, additional research focusing on refining the wake expansion and turbulence intensity parameters is recommended. Such improvements could potentially address some of the shortcomings identified in the current methodologies.

Sammendrag

Havvind sektoren er i vekst og det er derfor behov for pålitelige analytiske modeller for å kunne gevinstrealisere energiproduksjon. Denne rapporten vil bruke Python-modulen PyWake til å simulere og vurdere den årlige energiproduksjonen (AEP) for Dudgeon havvindpark fra en ett-, 10- og 20-års datasamling. Resultatene sammenlignes mot faktiske produksjonsdata fra året 2019-2020, innhentet fra Equinor. Vindkarakteristikker for Dudgeon har blitt hentet fra den åpne kilden Nora10. Anholt havvindpark brukes som et testtilfelle for å sammenligne funn fra simuleringene. Studien vil utforske hvor aktuell Weibull estimeringen er i forhold til en representasjon av vindhastighet i PyWake sin Bastankhah Porté-Agel simuleringsmodell, ved å analysere avviket i AEP. Videre vil optimaliseringsalgoritmene MLE- og L-BFGS-B bli brukt til Weibull-regresjonene som sammenligning av forskjellige regresjonsverktøy.

PyWake-modulen tilbyr et utvalg av scenario-baserte modellkombinasjoner, som kan defineres til brukerens spesifikke formål. Modulen består av tre hovedobjekter, som er sted-, turbin- og vakemodel. Vindparkmodellen som brukes i denne rapporten er en kombinasjon av den uniforme Weibull-site modellen og Bastankhah Porté-Agel vakemodell, med turbin- og steds parametere som er spesifisert til Dudgeon- og Anholt-tilfellene. Vakemodellen er kun anvendelig for lange vake tilfeller, og ser derfor bort fra påvirkningen av turbulensintensitet og bruker en konstant vakeekspansjons faktor. Stedsobjektet bruker den uniforme Weibull-modellen for å simulere AEP i samarbeid med vakemodellen. Den bruker form- og skala parametere fra tolv Weibull-sannsynlighetsfunksjoner fra tolv vindretningssektorer på 30°. Stedsobjektet krever også en sannsynlighet for forekomst av vindretning for hver vindsektor, som beregnes gjennom en sannsynlighetsmodell (KDE). Den statistiske passformen for Weibull-regresjonen vurderes ved hjelp av Kolmogorov–Smirnov-testen (KS test). Resultatene tolkes basert på KS-stat og p-verdien, og i forhold til AEP-resultatene.

Simuleringsresultatene avslører at størrelsen på datasamlingen har en betydelig påvirkning på nøyaktigheten av simuleringen. Ved bruk av en datasamling på ett år, ga L-BFGS-B-metoden de mest nøyaktige resultatene, med et avvik på bare 1,47 % fra de faktiske AEP-dataene. I motsetning, med en 20-års datasamling, viste MLE-metoden et mindre avvik på 0,8367 %. KS test resultatene viste at større datasamlinger produserte en lavere KS-stat, noe som indikerer en nærmere likhet med det faktiske vindhastighets-distribusjonshistogrammet. På den andre siden resulterte mindre datasamlinger i en statistisk likhet der p-verdien overskred 0.05, noe som tyder på en akseptabel passform under det brukte signifikansnivået. Videre ble AEP for hver vindretningssektor analysert individuelt. Resultatene viste varierende avvik for alle scenarier, og indikerer å ha en korrelasjon med KDE-regresjonen.

Denne studien viser klart at bruk av MLE metoden med større datasamlinger er å foretrekke for å oppnå pålitelige årlige energiproduksjonsprognoser. Derimot viser en ettårs datasamling at L-BFGS-B-metoden overgår alternativene. Ytterligere analyse avslørte også at KDE ikke er en effektiv metode for å dele sannsynligheten for forekomst på tvers av vindretninger. Regresjonsresultatene antyder at KDE ikke gir en nøyaktig indikasjon på sektorspesifikk AEP. For å forbedre studiens pålitelighet anbefales ytterligere forskning med fokus på utbedring av vakeekspansjonen og turbulensintensitetsparametere. Slike forbedringer kan potensielt adressere noen av manglene som er identifisert i de nåværende metodene.

List of Abbreviation

Abbreviation	Definition
AEP	Annual Energy Production
cdf	Cumulative Density Function
KDE	Kernal Density Estimation
KS-test	Kolmogorov-Smirnov test
L-BFGS-B	Limited-memory Broyden-Fletcher-Goldfarb-Shanno Bounds
MLE	Maximum Likelihood Estimation
MOM	Methods of Moment
NOJ	Niels Otto Jensen
NORA10	Norwegian Reanalysis 10 km
pdf	Probability Density Function
P-value	Probability value to evaluate hypothesis
SWT	Siemens Wind Turbine
TI	Turbulence Intensity
WD	Wind Direction
WS	Wind Speed

List of Symbols

$\overline{U}$	Mean wind speed
ρ	Air density
σ_U	Standard deviation
A	Rotor area
a	Shape factor
C_P	Power coefficient
C_T	Thrust coefficient
D	Width in rotor diameter
D_w	Wake expansion width
E_{tot}	Total energy
f	Weibull factor
k	Scale factor
k^*	Wake expansion rate
N	Amount
P	Power
r_0	Radius of the wake
t_i	Yearly hours
U	Wind speed
U_∞	Free stream wind velocity
U_w	Velocity in the wake
X	Distance downstream
x	Iterated value for Weibull

1 Introduction

With the global focus towards a green transition, aiming to reduce carbon emissions and combat climate change, the offshore wind sector is expanding in unison. The market potential in wind energy has had an exponential increase the last two decades for both onshore and offshore [1]. In line with the growth of the offshore wind farm sector, there is an increasing need for reliable analytical models to realize the energy production potential.

The objective with this thesis is to investigate the viability of using Weibull probability density functions as a representative wind speed distributions in simulation models. The properties of Weibull functions closely resemble those of a typical wind speed distribution histogram and are often used in simulation models to reduce computational load compared to time series analysis. Given that the Weibull curve is an approximation tool, it is desirable for the deviation from the production results to be as small as possible.

The report utilizes the Python module PyWake to perform simulations for the Dudgeon and Anholt wind farms, and compares the results against production data from Dudgeon. Two Weibull algorithms, Maximum Likelihood Estimation (MLE) and Limited-memory Broyden-Fletcher-Goldfarb-Shanno Bounds (L-BFGS-B), are used in combination with a kernel density estimation in Bastankhah Porté-Agel's wake deficit model. The Kolmogorov-Smirnov test (KS test) is performed as a goodness-of-fit test for the Weibull regression and is used in combination with simulation results to conclude the viability of using Weibull-represented wind speeds.

2 Theory

This section will introduce theory necessary to investigate the impact of wake in wind farms as well as how annual energy production is calculated, using simulations in the Python module PyWake. It is important to understand how a small deviation in parameters can induce relatively large variations in a wind farm's annual energy production. The section further explains the physics behind how wakes occurs and develops in addition to the relevant engineering models used to compute wind data parameters. Information about the selected wind farm sites and methods used for visual and computational analysing are also presented.

2.1 Wakes and PyWake

When a wind turbine converts the winds kinetic- into mechanical energy, conservation of energy results in a reduction of the wind speed downstream of the turbine. The air downstream of a turbine will have a higher turbulence compared to free stream, and is referred to as the wind turbine wake. The wake is influenced by the wind turbines characteristics, such as the blade aerodynamics, number of blades and the rotor diameter. According to Moskalenko et al. the energy losses due to wake effects in a wind farm are around 12 % [2]. Which is consistent with other literature, indicating that wake effect leads to average power losses of 10- to 20 % of the total power. [3, 4, 5]

The wake is divided into three different categories: near wake, intermediate wake and far wake. In Figure 2.1 the different categories are illustrated. Where the near wake is defined from the region close to the wind turbine, and two rotor diameter lengths downstream. Beyond this area is a transition region of two to five times the rotor diameter, referred to as the intermediate wake, which further leads to the far wake region. In this region the wake is fully developed, which means that the wake has reached a point where the velocity and turbulence approaches a Gaussian shape. [6, 4, 7, 2]

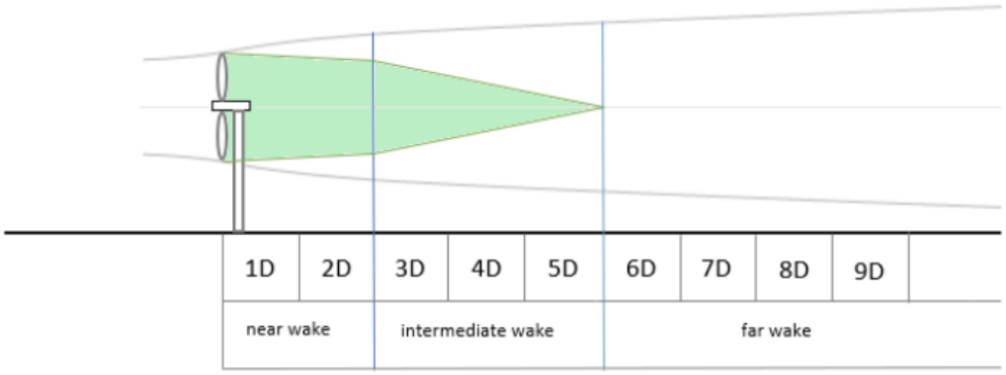

Figure 2.1: Schematic of wake. [6]

The wakes influence in an offshore wind farm is visualised in Figure 2.2 where the wake is observed due to special atmospheric conditions that created these fog wakes at Horns Rev 1 wind farm. [8]

Figure 2.2: Wakes in Horns Rev 1 wind farm, Denmark. [8]

2.1.1 PyWake

PyWake is a Python module developed by the Technical University of Denmark in order to better understand and predict the physiological behavior of wind farms. The PyWake module has the purpose of computing and simulating physics behind wind farms by using different engineering models and commercial plugins. In this report, PyWake is used to simulate the wake effect on wind turbines and AEP potential from two wind farms. [9]

PyWake offers a range of different modeling tools which can be combined to simulate most relevant wind farm scenarios and the respective AEP. These engineering models consisting of objects, such as site-, wind turbine- and wind farm model object. The site object defines the wind farm layout, with parameters for the number of turbines and their respective location. The wind turbine object takes in parameters for the turbine height, rotor diameter, power curve and thrust coefficient curve. Lastly, the wind farm model object defines which wake deficit models to include in the simulation. [9]

2.1.2 Bastankhah Gaussian deficit

The Bastankhah Gaussian deficit wake model is an analytical wake model proposed to predict the wind velocity distribution downstream of the wind turbine. The model is valid in the far wake and was first introduced by Majid Bastankhah and Fernando Porté-Agel in 2014, and will from now on be referred to as the Bastankhah Porté-Agel model. This model gives an understanding of the far wake behavior, to improve the accuracy of the wake predictions in the far wake region and builds further on the Niels Otto Jensen (NOJ) model. [7, 9]

The NOJ model is one of PyWake's wake deficit models. It operates on the principles of momentum conservation and assumes a linear wake distribution in terms of a top hat velocity deficit profile. It focuses on the far wake downstream from the wind turbine, where near wake effects are considered negligible. The velocity in the wake, U_w, is defined in Equation 2.1. U_∞ is the free stream wind velocity, r_o is the radius of the wake, X is the distance downstream and k^* is the wake expansion rate. [10]

$$U_w = U_\infty \cdot \left(1 - \frac{2}{3}\left(\frac{r_o}{r_o + k^* X}\right)^2\right) \tag{2.1}$$

Building on the foundations of the NOJ model, Bastankhah Porté-Agel has a more parabolic approximation to the far wake deficit, and is more based on a Gaussian profile. Over a distance, the turbulence intensity in the far wake region will vanish due to turbulent diffusion of the wake. [4]

Figure 2.3 presents the top hat model proposed by NOJ. Figure 2.4 illustrates the Bastankhah Porté-Agel wake model. U_∞ represents the free stream wind speed. U_w represents the reduced wind speed within the wake. The figures on the right, shows the wind speed deficit $(U_\infty - U_w)$, presenting the Gaussian distribution of reduced wind speeds of the turbine. Whereas the left figures show the NOJ top hat model. [7]

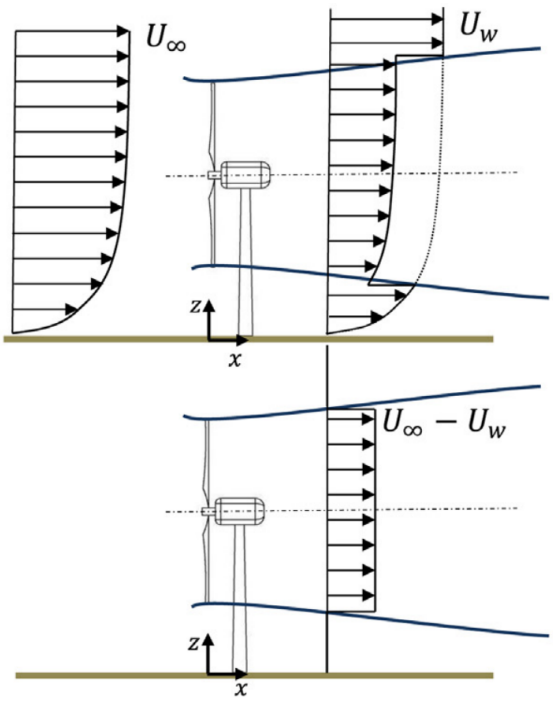

Figure 2.3: Vertical profiles of mean velocity (top) and velocity (bottom) downstream; top hat. [7]

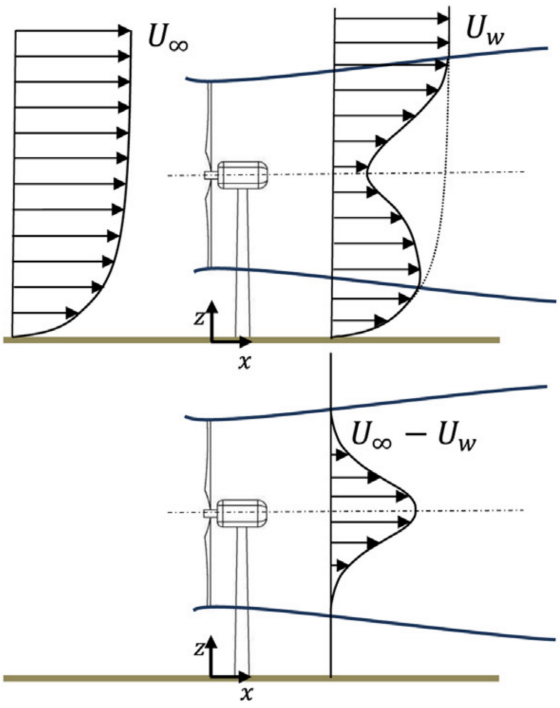

Figure 2.4:
Gaussian distribution for the velocity deficit in the wake. [7]

2.1.3 Turbulence intensity

The turbulence intensity (TI) is used as an approximation factor for wind turbulence used in wind related applications, and is an attempt to quantify the turbulence strength. Applying the variations of TI to simulation models, helps to further improve the predictions of power production. Turbulence intensity is calculated using the formula shown in Equation 2.2,

$$TI = \frac{\sigma_U}{\overline{U}} \tag{2.2}$$

where, over a given time frame, σ_U is the standard deviation in wind speed measurements, and $\overline{U}$ is the mean wind speed. [11].

2.1.4 Wake expansion

Figure 2.5 illustrates the wind turbines wake expansion downstream. The gray shading presents the volume in linear downstream condition, with the horizontal wake centre line being the dashed black line at hub height. The wake expansion width D_w shown as $n \cdot D$ in the figure, can be expressed as $D_w = D + 2k^*X$, where D is the initial wake width, k^* is the wake expansion factor and X is the downstream distance. [12]

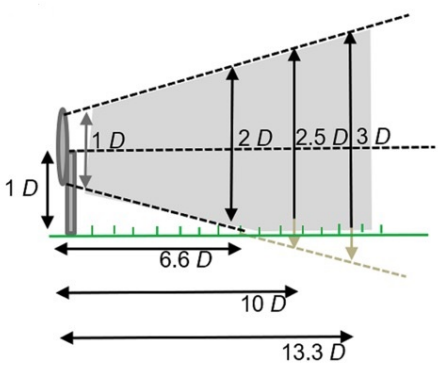

Figure 2.5: Wake expansion. [12]

The wake expansion rate (k^*) in a two-dimensional simulation depends on the variable chosen to characterize the velocity deficit profile. It can be challenging to evaluate, with little prior knowledge about the standard deviation in the wake expansion of turbine wake, such as Bastankhah Porté-Agel's definition of the expansion rate $k^* = \delta\sigma/\delta X$ [13]. Other wake models such as the NOJ model, have through research and applications led to a recommended value of $k^* = 0.05$, but is often criticised for its simplistic approach from a top hat velocity deficit profile [13]. A more appropriate approach to the Gaussian velocity profile is to express the wake expansion rate as a function of the turbulence intensity. Such that $k^* = 0.003678 + 0.3837TI$ for turbulence intensity values in the range $0.065 < TI < 0.15$ [14].

PyWake utilizes applications from a new analytic model for wind turbine wakes, and obtains the wake by applying mass and momentum conservation [7]. The standard value of the wake expansion factor is set to $k^* = 0.0324555$, based on a turbulence intensity of 0,075 for most Gaussian wake model examples, but recommends the user to evaluate a new k^*-value based on the turbine and site variables. [9, 15]

2.2 Annual Energy Production

Annual energy production is a measurement of the gross total energy produced in the fraction of a year and is the basis for economic valuation of a wind farm [16]. A wind farm operation includes seven different loss categories. These include wake loss, availability, turbine performance, electrical, environmental, curtailment and others [17].

The power in the wind P, is given by equation 2.3 where ρ is the air density, A represents the wind turbines rotor-area and U as the wind speed. C_p is an expression for the wind turbines efficiency [18]. From this formula it is clear that a reduction in wind speed will affect the power produced.

$$P = \frac{1}{2}\rho U^3 A C_p \tag{2.3}$$

Further the AEP can be obtained from equation 2.4 .Since P is dependent on the wind velocity and varies with time, the power can be expressed as a function of time. Hence E_{tot} is the energy produced for a given time period. The AEP will therefore be the sum of all different values of power extracted by the turbine through the year. [18]

$$E_{tot} = \int_{t_1}^{t_2} P(t)dt \approx \sum_{i=1}^{N} P_i \cdot \Delta t_i \tag{2.4}$$

2.3 Wind direction and wind speed

Time series analysis is a specific way of analyzing a sequence of data points over an interval of time. It is used to understand the underlying causes of trends or systematic patterns over time. Using the data visualization, it is possible to see trends and find out why and how these trends occurs. [19]

The wind is well known as an intermittent energy source with variations regarding direction and speed. In this report, the North-direction will be referred to as 0°, with the other directions referred to as in Figure 2.6. The wind characteristics varies with distance from shore and there are in general higher wind speeds further towards offshore sites, still there are exceptions depending on the local conditions. [20]

A wind rose diagram gives a simple description of the wind direction and magnitude. An example of how a wind rose looks is given in Figure 2.6. The colors are labeled to different wind speeds and the arrows indicates that the wind blows towards the center of the rose. [21]

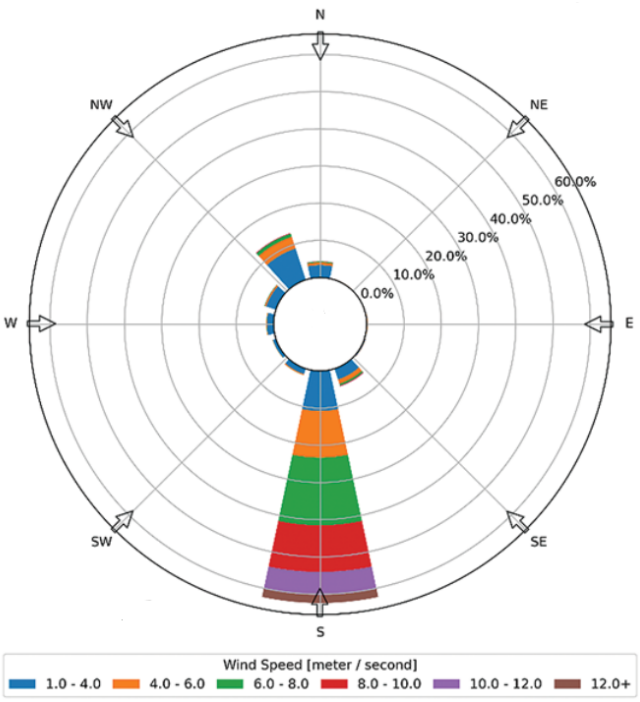

Figure 2.6: Example of wind rose layout. [21]

Histogram is a chart type that presents the frequency distribution of data points across a range of numerical values. The data are grouped into interval ranges known as bins, that are arranged in consecutive order along the horizontal x-axis. The height of each bar extends vertically along the y-axis, representing the number of data points within each bin [22]. Figure 2.7 illustrates an example of a histogram that uses probability for wind speed. Each bar covers a wind speed of one m/s, and the height indicates the probability of each time range. [23]

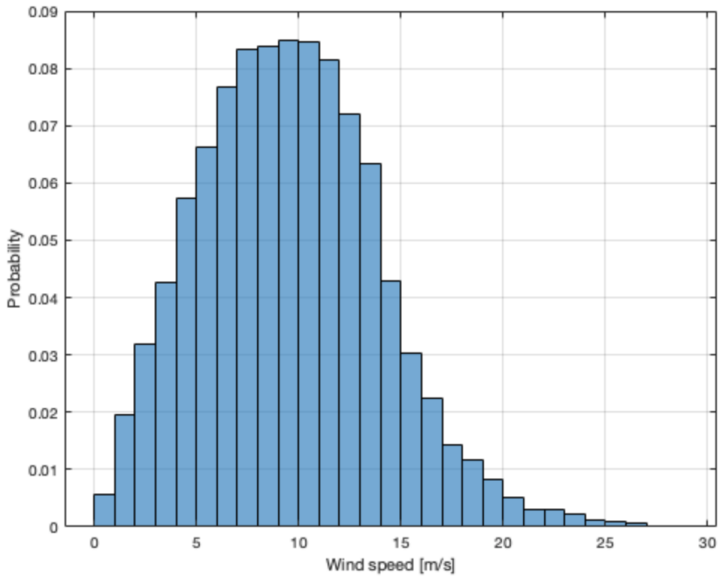

Figure 2.7: Example of histogram. [23]

2.4 Site Object

To access the wind energy potential at the locations of Dudgeon and Anholt, the site object in PyWake provides information for the analysis of the wind characteristics. It includes measurements of wind speed (WS), wind direction (WD) and turbulence intensity. As stated in PyWake: "The site object is responsible of calculating the down-wind, cross-wind and vertical distance between wind turbines" [9].

2.5 Weibull distribution

The Weibull distribution is a commonly used probability model for estimating wind speeds in a wind farm site in the form of a histogram regression. The Weibull regression is an asymmetric distribution, skewing towards the bulk of the distribution. By utilizing this model, it is possible to parameterise a probability density function (pdf) with only two parameters, shape and scale. The shape and scale parameters are used as inputs in wind farm simulations. With the wind speed represented as a function of probability instead of a large number of metric data, the simulation will save computing time and processing power. In equation 2.5 the scale factor is represented as k, and shape factor as a. The variable x represents each data iteration. [24, 25]

$$f(x;k,a) = \frac{k}{a} \cdot \left(\frac{x}{a}\right)^{(k-1)} \cdot e^{-(\frac{x}{a})^k} \tag{2.5}$$

An example of how a Weibull distribution is shown in Figure 2.8 and Figure 2.9. In Figure 2.8 the distribution is plotted versus wind speed under a constant value of $a = 1$ and different values of k. As it can be seen by Figure 2.8, a higher value of k leads to a smaller variation in wind speed. [26]

Figure 2.9 shows a Weibull distribution density versus wind speed under a constant value of $k = 3$ and different values of a. The value of a scales the deviation in wind speed. The deviation is higher with a higher value of a. [26]

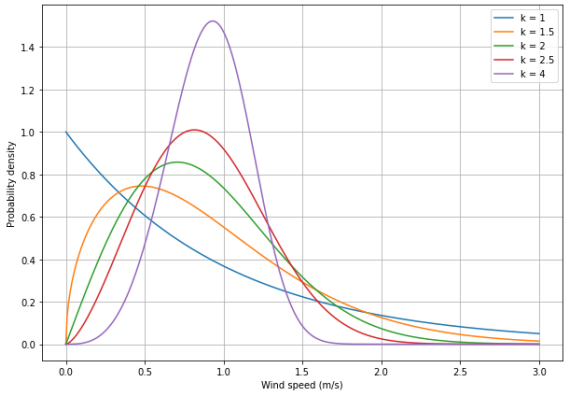

Figure 2.8:
Weibull distribution - different values of k.

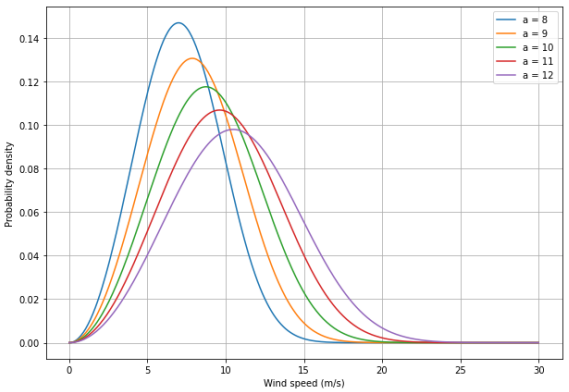

Figure 2.9:
Weibull distribution - different values of a.

2.5.1 Literature on Weibull

To get an understanding about which results that can be expected from this investigation, it is necessary to look into literature from previous studies. Wind speed distribution is frequently characterised through a Weibull distribution, as it is a good approximation for many cases and used in order to obtain a mathematical function for wind speed simulation models [25]. Based on results from previous studies, the suitability of the different algorithm methods varies with the samples data size, format, distribution and goodness-of-fit test [25]. Least Square Technique (LST), Method of Moments (MOM), MLE and Limited-memory Broyden-Fletcher-Goldfarb-Shanno Bounds (L-BFGS-B), are methods proven to be sufficient for estimating the Weibull parameters in wind farm simulations [25, 27, 28, 29]. MLE has in studies shown as the most efficient method regarding Weibull estimations for power density [27, 30]. Whereas L-BFGS-B is a gradient based method, which means the method uses knowledge about the gradient of the wind farm layout . L-BFGS-B is a method with fast performance, but not the best results regarding AEP calculations.[31, 32, 33]

There are two functions that characterizes the variation in wind speed in a Weibull distribution, the probability density function which indicates the probability for which the wind occurs at a given wind speed. And the cumulative distribution function (cdf), that gives the cumulative probability of observed wind speeds. [25, 26]. Based on previous studies it is clear that the best method to estimate the Weibull parameters varies with different sites and is dependent on each situation. [24, 27, 30, 26, 34, 35]

2.5.2 Approaches to Weibull fitting

In this section the different approaches to Weibull fitting is explained. This thesis will proceed with the MLE- and the L-BFGS-B method. With the two methods it will be possible to compare the results and analyze any differences or similarities from both algorithms.

2.5.3 Maximum likelihood estimation

With the use of MLE the goal is to find the optimal way to fit the Weibull distribution to the collected data. This method finds the optimal value of the mean in observed measurements and is defined as where the slope is equal to zero. The method is an important tool for non-linear modeling, such as for Weibull regression. [36, 37]

Sufficiency, consistency and efficiency are some of the optimal properties the MLE-method has regarding estimation. MLE is simplified by using the logarithmic of the function since the peak values are the same for both log-likelihood- and likelihood function. With this step the derivatives will be easier to perform [38]. By using iterative steps, this method aims to identify points where the probability distribution makes the observed data most probable in comparison to the original data sample. [36, 39]

2.5.4 L-BFGS-B method

L-BFGS-B is a variant of standard BFGS-methods, where the L stands for limited memory and the B describes that the method includes bounds on the variables. The L-BFGS-B method is intended to solve for large heavily problems or where the Hessian matrix is challenging to acquire. Instead the algorithm approximate the matrix such as the required storage is linear to the number of variables [40]. It is a "quasi-Newton algorithm for solving large non-linear optimization problems with simple bounds on the variables." [40]. The methods advantage is not necessary to maintain knowledge about the objective functions structure. [40]

The method is relevant for use in wind farm simulations for several reasons. Because of its fast computational time, the Weibull parameters can be obtained efficiently by finding the values which fits the data according to some objective function. L-BFGS-B is able to handle constraints naturally and ensure that the solutions are feasible to real conditions, in example the turbines placement. When performing wind farm simulations, large datasets with many variables is examined. The method's memory-efficiency is beneficial in such cases, allowing for optimization without excessive computational resource requirements. [28, 41]

2.6 Kolmogorov-Smirnov test

The Kolmogorov-Smirnov test is used to decide whether two different samples is likely to exist of the same distribution. It is a non-parametric statistic test, which is useful when the distribution is not normally distributed . To evaluate whether the distributions are close to similar, a hypothesis testing is performed. The KS test uses the maximal difference between the two distributions to decide if the null hypothesis can be discarded or not. The null hypothesis can be defined as the distribution consist of the same fit. To conclude the outcome of the KS test, the p-value evaluates the statistical resemblance between the two samples. A p-value lower than a significance level at 0.05 results in rejection of the null hypothesis. Which will indicate that the distributions are likely to not originate from the same sample. A higher p-value indicates a higher statistical probability of two distributions, originating from the same sample. Additionally a KS-stat value from the test, is the value of the maximum distance between two points from the same iteration index. The KS-stat indicates how two distributions deviates from each other, where a low value indicates a close resemblance and a high value could indicate a poor resemblance. Still, there are instances where a high KS-stat could originate from outliers from the statistical test, and should be interpreted carefully. [42, 43, 44, 45]

Figure 2.10 is an example of how the KS test converts the data to a cdf and iterates through each data point. The maximum difference between the histogram and pdf is presented with the KS-stat value. [46]

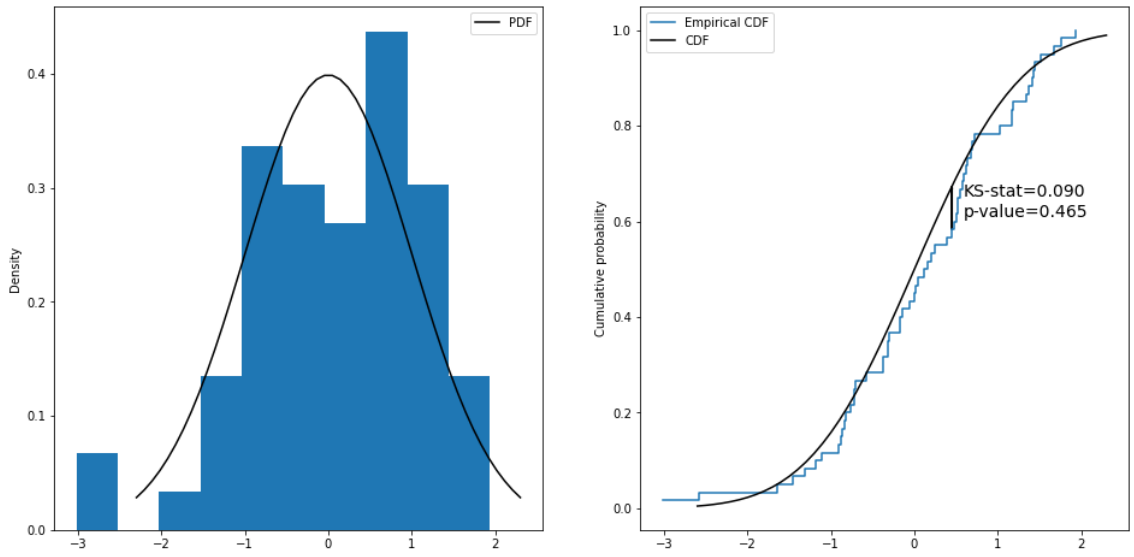

Figure 2.10: Example of KS-test. [46]

3 Method and Materials

Collected data is presented in the form of a histogram which is compared with a Weibull distribution. To check whether the Weibull distribution is representative of the real data, the Kolmogorov-Smirnov test (KS test) is used. Finally, the results from the various locations are compared to see if there is a large variation in the estimations.

3.1 Wind and production data

The data used in the wind farm simulations for the Dudgeon site was provided by Equinor. The Anholt weather data was imported from Ørsted's homepage as an open source data file [47]. Both companies have open source information about the turbine dimensions for each location.

The Dudgeon data consist of turbine locations, production data for the period 2019 to 2020 and a time series of weather data from Nora10. The production data is provided in a filtered and unfiltered version, where the unfiltered data is presented in Table 3.1. The report will take basis in the unfiltered data version, as the PyWake simulations do not disregard insufficient operating conditions to the same degree as the filtered data file from Equinor. Additionally in regards to Weibull fitting and wake deficit models, sub standard wind speeds and power production, should be included to encompass all scenario conditions.

Table 3.1: Production data and wind data, Dudgeon

	Production data, Unfiltered	**Wind data**
Source	Equinor	NORA 10
Variables / Inputs	ws, wd, std ws, power	ws, wd
Measurement height	Hub height	100m
Interval	10 min	3 hours
Time Period	2019 - 2020	2002 - 2022
Total Sample Size	3 518 731	58 400

The Anholt weather data is for the year 2013-2014 and shown in Table 3.2. No production data or turbine locations from Anholt were obtainable from the wind farm operator. The relative turbine locations required in the site object were obtained using the plotting tool "PlotDigitizer" over a turbine layout graphic from literature [48]. Since no production data were available, the simulations at Anholt will be used as a test case, in order to determine a trend in Weibull approximations with regards to wind direction and sample size.

Table 3.2: Production data and wind data, Anholt

	Production data, Unfiltered	**Wind data**
Source	-	Ørsted
Variables / Inputs	-	ws, wd
Measurement height	-	80 m
Interval	-	10 min
Time Period	-	2013 - 2014
Total Sample Size	-	52 560

3.2 Dudgeon

Figure 3.1 presents a map illustrating the geographical location of the Dudgeon wind farm in the North Sea, at the east coast of England. The wind farm is situated in North Norfolk, approximately 32 kilometers north from the shore. Figure 3.2 presents the layout of the Dudgeon wind farm, providing with a detailed view of how the wind farm is structured. The nearest neighbouring wind farm Sheringham Shoal is located approximately 10 kilometers southwest of Dudgeon. [49]

Figure 3.1:
Geographical map, Dudgeon. [50]

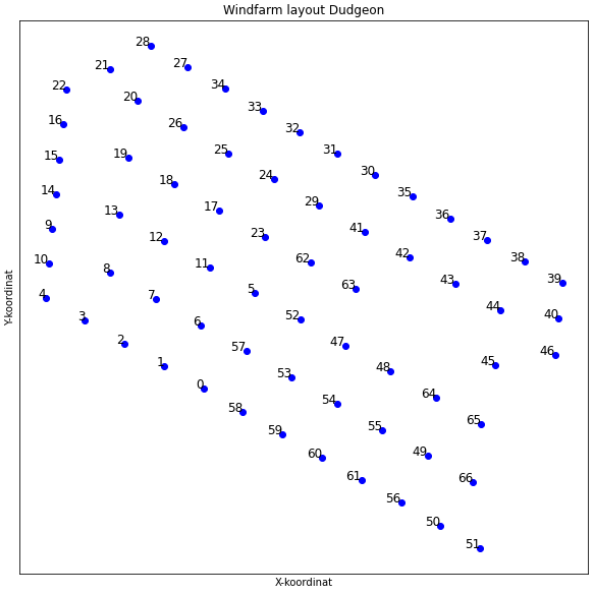

Figure 3.2:
Layout of Dudgeon, England.

Table 3.3 provides detailed information from the site of the Dudgeon wind farm. Each of the 67 Siemens SWT 6.0-154 turbines is located in Dudgeon, and has a diameter of 154 m with a hub height of 103 m. It is producing a total installed capacity of 402 MW, with each turbine producing 6.0 MW as shown in the table. [49, 51, 52, 53]

Table 3.3: Detailed site information for the Dudgeon wind farm [49, 51, 54, 55, 56]

Site information	
Site	Dudgeon
Location	North Norfolk, England
Wind Turbines	Siemens, SWT 6.0-154
Total turbines	67
Diameter [m]	154
Hub height [m]	103
Water depth [m]	18-25
Distance from shore [km]	32
Wind turbine capacity [MW]	6.0
Installed capacity [MW]	402
Owner	Equinor 35%, Masdar 35% and China Resources 30%

3.3 Anholt

Figure 3.3 presents a map illustrating the geographical location of the Anholt wind farm, east coast of Denmark. The wind farm is situated in Kattegat approximately 15 kilometers from shore. Figure 3.4 presents the layout of the Anholt wind farm, and how the wind farm is developed. A greater version of Anholt's layout is to be found in Appendix A. [57]

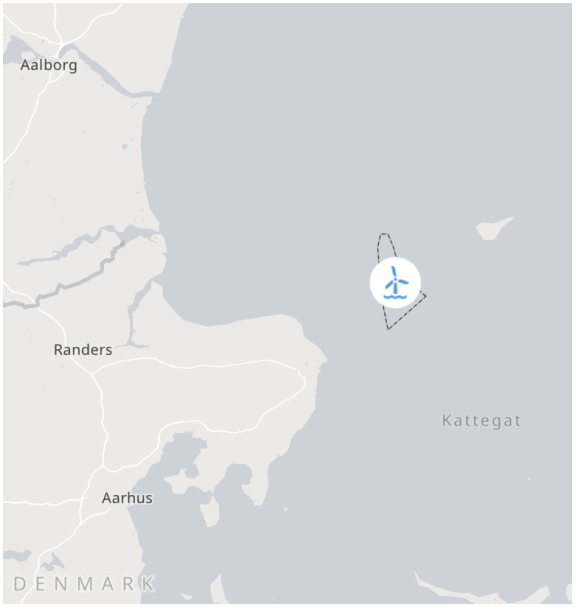

Figure 3.3:
Geographical map, Anholt. [58]

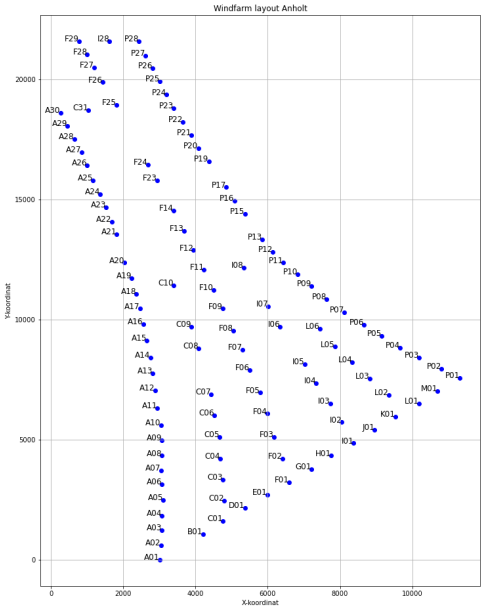

Figure 3.4:
Layout of Anholt. [48]

Table 3.4 provides detailed site information from the Anholt wind farm. It is a total of 111 Siemens, SWT 3.6-120 turbine with a diameter of 120 m with a hub height of 81.6 m. It is a total of 111 turbines with an installed capacity of 400 MW. [57]

Table 3.4: Detailed site information for the Anholt wind farm [57]

Site information	
Site	Anholt
Location	Between Djursland and Anholt, Kattegat outside of Denmark
Wind Turbines	Siemens, SWT 3.6-120
Total turbines	111
Diameter [m]	120
Hub height [m]	81.6
Water depth [m]	15-19
Distance from shore [km]	15
Wind turbine capacity [MW]	3.6
Installed capacity [MW]	400
Owner	Ørsted 50%, PensionDenmark 30% and PKA 20%

3.4 Power curve and thrust coefficient

Table 3.5 presents a comparison of power curve and thrust coefficient values for the wind turbines used at the two locations; Anholt and Dudgeon. At Dudgeon the installed wind turbine is SWT 6.0-154, it is a Siemens turbine with installed capacity at 6 MW with 154 m rotor diameter. The wind turbine at Anholt is also produced by Siemens, but have an installed capacity of 3.6 MW and 120 m rotor diameter, hence the name SWT 3.6-120.

Table 3.5: Comparison of power curve and C_T values for Dudgeon and Anholt

Wind Speed	**Power [kW]**		C_T	
[m/s]	**Dudgeon**	**Anholt**	**Dudgeon**	**Anholt**
3.0	0	0	0.77	0.0
4.0	220	161	0.77	0.86
5.0	440	351	0.76	0.86
6.0	721	635	0.76	0.86
7.0	1173	1026	0.77	0.86
8.0	1796	1544	0.76	0.86
9.0	2517	2204	0.76	0.86
10.0	3360	2910	0.69	0.80
11.0	4485	3399	0.61	0.61
12.0	5792	3567	0.43	0.42
13.0	6000	3596	0.33	0.32
14.0	6000	3600	0.26	0.25
15.0	6000	3600	0.21	0.20
16.0	6000	3600	0.17	0.17
17.0	6000	3600	0.14	0.14
18.0	6000	3600	0.12	0.12
19.0	6000	3600	0.10	0.10
20.0	6000	3600	0.09	0.09
21.0	6000	3600	0.08	0.08
22.0	6000	3600	0.07	0.07
23.0	6000	3600	0.06	0.06
24.0	6000	3600	0.05	0.05
25.0	6000	3600	0.05	0.05

3.5 Simulations

Since this report focuses on the accuracy of a Weibull simulated AEP, the wind farm model is defined to only include a wake deficit model. This is due to difficulties obtaining various information about the two wind farms, and hence one loss category will better maintain simplicity and continuity throughout the research. The engineering wind farm model used in this report are based around the Bastankhah Porté-Agel wake deficit model, which is valid for far wake simulations and rely on a uniform wind distribution. The model has the option of simulating for both time series data, and Weibull functions. Bastankhah Porté-Agel simulates wind speeds as a uniform "gust" of wind represented as the mean wind speed in ten minutes intervals over the entire farm site. Due to the excessive work needed in order to determine the correct wake expansion factor the report will move on with PyWake's standard value of $k^* = 0,0324555$, but with the insight that an estimated value of k^* have an expected influence on simulation results. Additionally, the model disregards the effect from turbulence intensity. Simulations will be performed for the one-, 10- and 20-year time periods for Dudgeon. Anholt will be simulated for one time period of the year 2013-2014.

3.5.1 Time series simulation

The time series simulations implements vector variables for turbine location, wind direction, wind speed, turbulence intensity and time span for each time series data point. Time series simulations are performed for both Anholt and Dudgeon, where previously mentioned, Anholt is simulated with ten minute intervals and Dudgeon with three hour intervals. For comparison purposes, it is performed a simulation for each site over a one-year period, in order to cross examine the accuracy of Weibull simulations with time series for both locations.

3.5.2 Histogram and wind rose

All wind speed and direction data are plotted in a histogram chart as a function of frequency, in order to further determine the spread and probability of occurrence as shown in Figure 3.5. This is done for twelve sectors, determined by the wind direction. The sectors are slices of a full circle with 30° intervals, where the first sector (sector 0) ranges from 345° to 15° shown in Figure 3.6. The sectors are labeled from sector 0 to sector 11. Each histogram is plotted with 25 bins, with the bin centering being the mean of the bin edges. The number of bins were chosen to best represent a bin width of 1 m/s, as the wind data contains very few wind speeds over 25 m/s. The number of bins should be representative to the range in wind speeds and the number of wind measurements. For this report, 25 bins is deemed sufficient because of the large data samples, and because a smaller number of bins also saves computational time of the simulations.

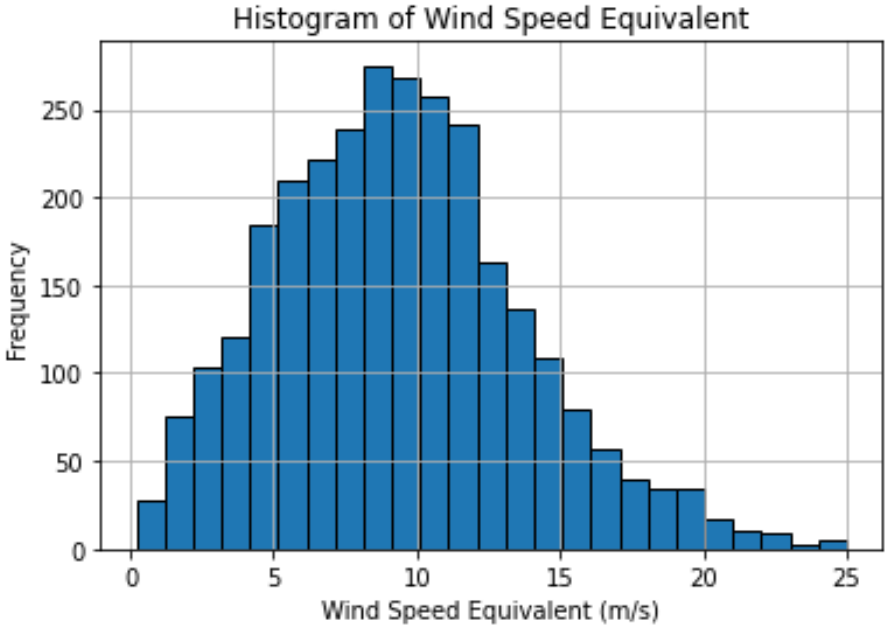

Figure 3.5: Histogram, frequency of wind speed, Dudgeon.

In Figure 3.6 the wind rose for all cases are shown. In the two upper wind roses represents Anholt and Dudgeon with the one-year sample. The wind roses at the bottom shows the wind direction data for 10- and 20-year. As seen in the caption of the figure, the wind speed is represented with different colors. Blue, orange, green, red and purple corresponds to 0-5 m/s, 5-10 m/s, 10-15 m/s, 15-20 m/s and 20-25 m/s in respective order.

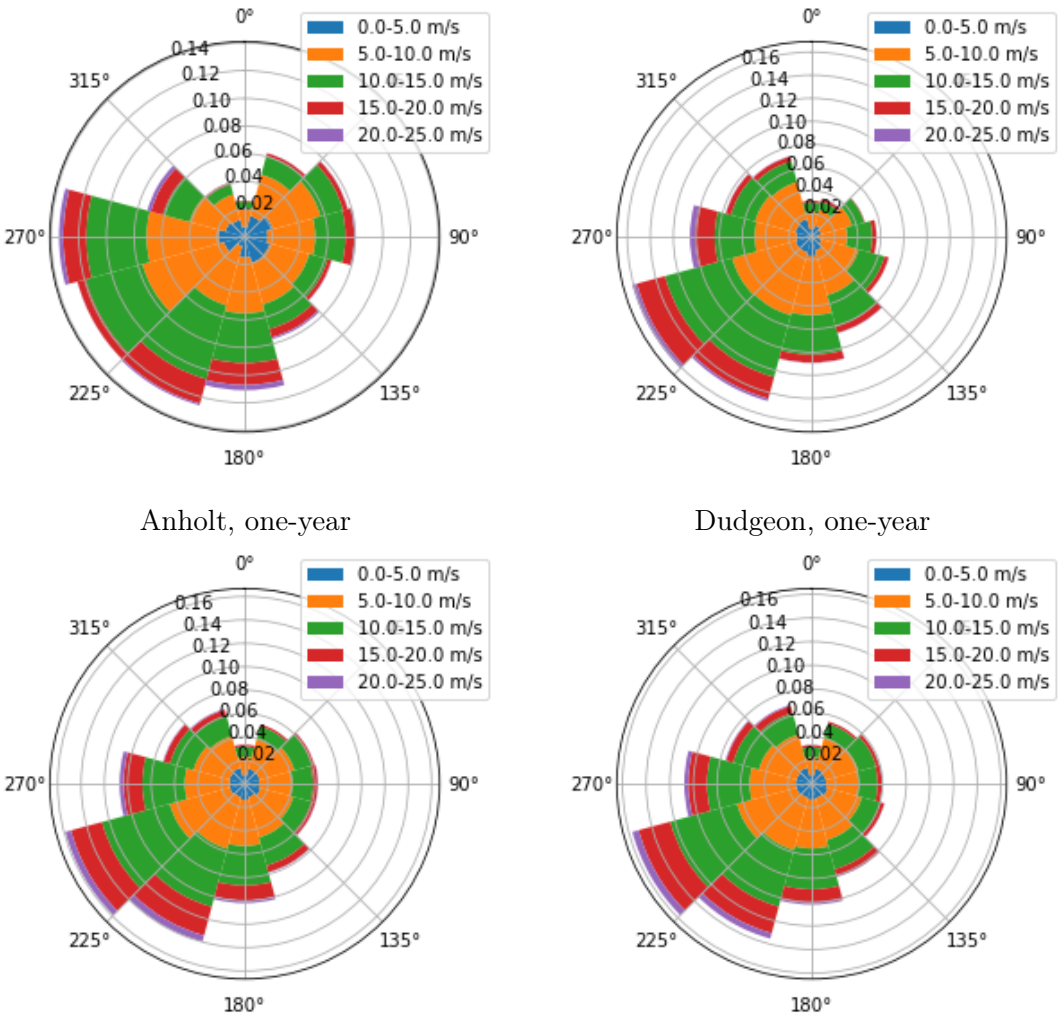

Anholt, one-year

Dudgeon, one-year

Dudgeon, 10 years

Dudgeon, 20 years

Figure 3.6: Wind roses, Dudgeon and Anholt for different time periods.

3.5.3 Weibull simulation

The Weibull simulation in the site object, notated as "UniformWeibullSite" and is based on Porté-Agel's Gaussian model, is a PyWake module that use pdf's for sector based wind speed and wind direction. Functions are parameterized with the use of the statistical function "scipy.stats" in Python, from the twelve histogram plots. The module uses the shape and scale factors as input parameters from the Weibull wind speed functions at each section.

The Weibull distribution functions are parameterized using the MLE (red curve) and L-BFGS-B (blue curve) method as shown in Figure 3.7. Both methods are relevant for wind farm simulations, where MLE is the most commonly used, and L-BFGS-B has advantages handling large data samples. Both methods are used in order to investigate if there are sectors where one method is more sufficient. As an extra step, it is performed a simulation to see if a combination of methods produces a more accurate AEP estimate when selecting the best statistical curve fit from each sector. Figure 3.8 shows the wind direction based on a kernel density estimation and is used in a probability of occurrence vector. The comparison of the data from Anholt and Dudgeon with shape and scale factors are presented in Table 3.6.

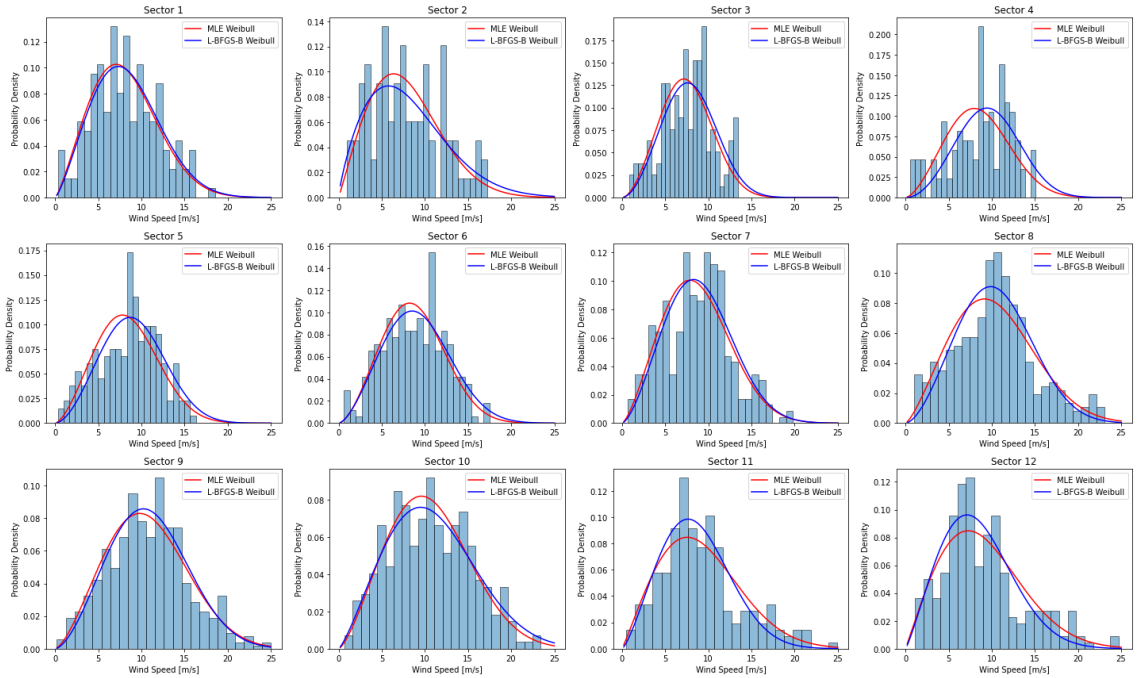

Figure 3.7: Weibull fitting with MLE and L-BFGS-B for each wind sector at Dudgeon 2019-2020.

Table 3.6: Data Comparison Across Different Methods and Time Periods

Sector	MLE				L-BFGS-B			
	Anholt 2013-2014		Dudgeon 2019-2020		Anholt 2013-2014		Dudgeon 2019-2020	
	Shape	Scale	Shape	Scale	Shape	Scale	Shape	Scale
Sector 0	2.34333	8.21829	2.26888	9.13542	2.26949	8.32611	2.30066	9.3784
Sector 1	2.41286	8.4352	2.04596	8.85722	2.24203	8.7216	1.79944	9.07404
Sector 2	2.19784	8.70015	2.79665	8.3938	2.0573	8.7098	2.85293	8.82591
Sector 3	2.16608	10.1284	2.61122	9.57484	2.12964	9.93498	3.02497	10.7943
Sector 4	2.01537	8.92557	2.57255	9.44247	1.9831	8.60506	2.76049	10.2253
Sector 5	2.06956	9.47624	2.66318	9.81359	1.88007	9.62261	2.59319	10.2806
Sector 6	2.25841	11.4943	2.42244	9.79248	2.24343	11.8112	2.5377	10.112
Sector 7	2.79586	11.7844	2.34265	11.6089	3.14155	12.3051	2.67872	11.7496
Sector 8	2.64262	10.0508	2.47602	12.0831	2.84553	10.2106	2.6305	12.2679
Sector 9	2.27969	11.241	2.41338	11.9691	2.29903	11.3293	2.26523	12.3041
Sector 10	1.98771	10.9893	2.07526	10.3756	1.91082	11.081	2.33533	9.71771
Sector 11	1.88262	8.64952	2.02158	10.1864	2.00601	8.14514	2.18027	9.45865

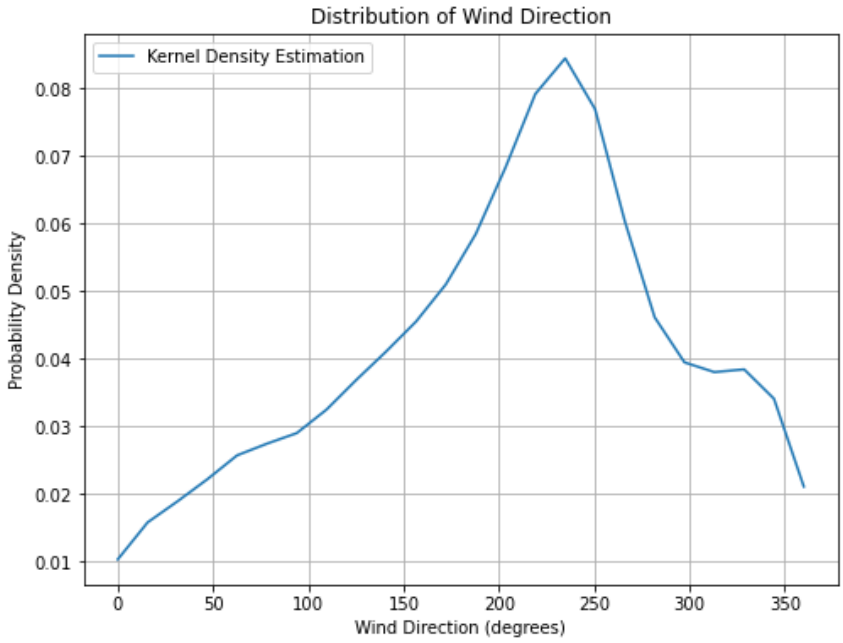

Figure 3.8: KDE wind direction - Dudgeon 2019-2020.

To maintain an anonymous approach of the production data provided by Equinor, all measurements and comparison are given as a percentage of the total AEP with the unfiltered data for Dudgeon wind farm. Table 3.7 shows the AEP division for each wind direction sector from the sourced Equinor data. Additionally the normalized probability of occurrence from the KDE regression of the open source Nora10 data for one-, 10- and 20-year data samples is presented.

Table 3.7: KDE values compared to wind sector AEP amount.

	Amount of production [%]	**Normalized KDE-values**		
Sector	**Unfiltered data**	**Dudgeon one-year**	**Dudgeon 10-year**	**Dudgeon 20-year**
Sector 0	5.9283 %	0.0313	0.0335	0.0329
Sector 1	2.6893 %	0.0346	0.0526	0.0544
Sector 2	3.4427 %	0.0478	0.0618	0.0593
Sector 3	4.2717 %	0.0563	0.0628	0.0599
Sector 4	5.0482 %	0.0693	0.0628	0.0638
Sector 5	6.6053 %	0.0865	0.0787	0.0814
Sector 6	8.4898 %	0.1094	0.1022	0.1022
Sector 7	16.7287 %	0.1474	0.1403	0.1358
Sector 8	21.9067 %	0.1613	0.1592	0.1575
Sector 9	11.8990 %	0.1064	0.1075	0.1082
Sector 10	6.8190 %	0.0774	0.0724	0.0756
Sector 11	6.1713 %	0.0724	0.0663	0.0691

3.6 KS test

In order to evaluate the statistical resemblance between the histogram and the Weibull regression, the goodness-of-fit KS test is performed. The KS test is a statistic function built-in python module which takes the different samples as input and computes the relevant values. The data is iterated through each wind speed in the histogram, where the center of the bin serves as the reference point between the Weibull regression and histogram. The foundation in the test is based on developing two hypothesis, beginning with defining the null hypothesis. In this case, the null hypothesis is defined as: there is no difference between the compared samples. The alternative hypothesis is defined as: the compared samples originates most likely from a different distribution. The significance level is chosen as 95 % in this thesis, similar to previous studies. A p-value lower than 0.05 will hence indicate a rejection of the null hypothesis, accordingly the compared samples do not follow the same distribution.

3.7 Wind sector analysis

To further determine the accuracy in AEP from Weibull simulations, the wind sectors will be compared individually with regards to the goodness-of-fit, ratio between simulated and actual energy production, and sample size. The number of acquisitions at each sector is shown in Table 3.8.

Table 3.8: Sample Sizes across Different Sectors

Sector	Dudgeon 2019-2020	Dudgeon 2012-2022	Dudgeon 2002-2022	Anholt 2013-2014
Sector 0	180	1894	3692	2589
Sector 1	98	1473	3079	3308
Sector 2	150	1824	3370	4110
Sector 3	141	1716	3316	3973
Sector 4	199	1700	3525	3184
Sector 5	239	2206	4581	3766
Sector 6	292	2816	5663	5710
Sector 7	400	3873	7415	6437
Sector 8	507	4633	9093	5988
Sector 9	287	3148	6392	7182
Sector 10	204	2074	4333	4205
Sector 11	223	1867	3941	2108
Total	**2 920**	**29 224**	**58 400**	**52 560**

Regardless of production, it is also valuable to examine trends from the KS test, and if or why there are some sectors where Weibull is better suited to estimate wind speed conditions. This comparison is performed for the one-, 10- and 20-year period in Dudgeon with the main focus on the sample size, as well as a comparison for the one-year scenario between Dudgeon and Anholt to also investigate similarities based on location.

3.8 Source of error and assumptions

Beside the stated disregards from theory, such as the turbulence intensity and wake expansion factor, there are several potential sources that could lead to errors. It is necessary to address the assumptions and acknowledge their impact on the results.

The analysed weather data is not collected at each turbine placement and will not include local wind data at each point in the wind farm. Because of this the simulated results may vary from the real world situation. Regarding the wind farms positioning, the influence from neighboring wind farms are not taken into account in this case. From theory it can be assumed that wakes from neighboring wind farms will have an affect on the inflow conditions. For instance the Sheringham Shoal wind farm, located southwest of Dudgeon and Sønderbjerg to the east of Anholt.

Additionally, PyWake's Bastankhah Porté-Agel method is applicable for far wake scenarios only. Based on the provided turbine layout information for Dudgeon, for many cases the turbines will categorise as intermediate- to far wake scenarios. The experience of wake for each turbine will vary depending on the wind direction, which is why the Bastankhah Porté-Agel model was chosen as a simplification.

The wind speed used for simulations are measured at a height of 100 meters and 80 meters for Dudgeon and Anholt respectively. The height is different than the turbine hub height, which can result in a slight deviation in wind speed. Another topic that can affect the production data, are maintenance and periods when the wind turbines are inoperative. None of the simulations include periods where the wind turbine is not operating. In addition there are not included power regulation during operational considerations. Based on this the simulation results will deviate from the real production data. It would therefore be reasonable to assume that the methods that overestimate with regard to AEP will be the methods that give a result most similar to the actual produced energy.

4 Results

This section presents the results from the simulations. The results are organized in a systematic approach beginning with results from three different time periods at Dudgeon. First introducing results from the total sample, followed by each individual wind sector, and then the one-year results from the Dudgeon and Anholt simulations respectively. Lastly the comparison between the different methods is presented regarding AEP.

4.1 Weibull fit to wind data at Dudgeon

The Dudgeon data is processed for three different time periods, a one-, 10- and 20-year data sample from Nora10. The MLE and L-BFGS-B method are applied to generate a Weibull distribution. In the first part the distributions depend on total wind speed data for all sectors. The sample sizes are presented in Table 3.8 in Section 3.7. Further in this section the plots for different sectors follows for each method.

4.1.1 Full data sample at Dudgeon with MLE method

The estimated Weibull distributions from the MLE method from the one-, 10- and 20-year time period in Dudgeon is presented in Figure 4.1. The red line represents the Weibull regression for the 2019-2020 time period. The blue line represents the 10 year period 2012-2022 and the green line the 20 year period 2002-2022. In addition the shape and scale parameters for each case is given in Table 4.1 and also values from KS test.

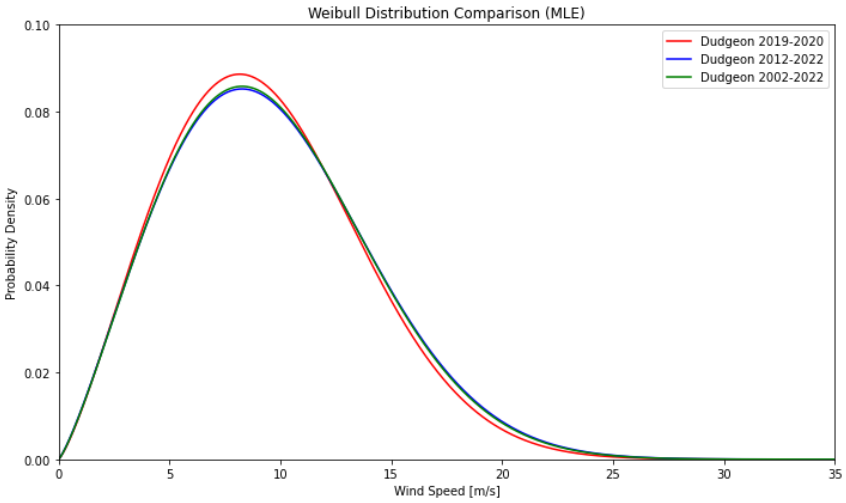

Figure 4.1: Weibull distribution for Dudgeon - MLE.

Table 4.1: MLE statistics for Dudgeon (one-, 10-, and 20 years)

MLE	Dudgeon, 1 year	Dudgeon, 10 years	Dudgeon, 20 years
KS-stat	0.0599	0.0153	0.0160
P-value	0.0117	0.2069	0.0000
Shape	2.2661	2.2231	2.2342
Scale	10.5628	10.8288	10.7934

4.1.2 Full data sample at Dudgeon with L-BFGS-B method

L-BFGS-B method from the one-, 10- and 20-year time period in Dudgeon is presented in Figure 4.2. The line color is represented in the same way as the plot for MLE method. The Weibull parameters and KS-test values from the L-BFGS-B method is seen in Table 4.2.

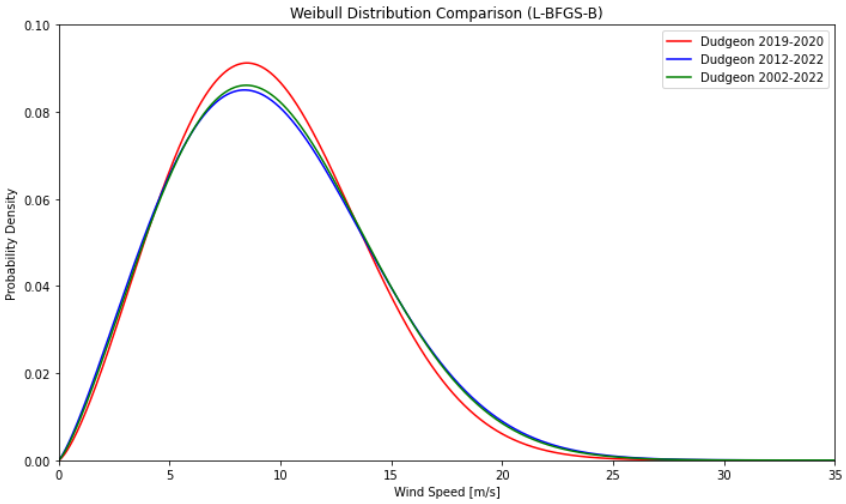

Figure 4.2: Weibull distribution for Dudgeon - L-BFGS-B.

Table 4.2: L-BFGS-B statistics for Dudgeon (one-, 10-, and 20 years)

L-BFGS-B	**Dudgeon, 1 year**	**Dudgeon 10 years**	**Dudgeon 20 years**
KS-stat	0.0765	0.0246	0.0153
P-value	0.1393	0.2069	0.3132
Shape	2.1803	2.0781	2.0896
Scale	9.4587	9.9600	10.1256

4.1.3 Wind sectors at Dudgeon with MLE method

Figure 4.3 displays four of the twelve Weibull-curves from the wind sectors. The colorization of the curves are similar as explained in Figure 4.1 and Figure 4.2. Due to the variability of wind direction, the sample size for the sectors also varies continuously. For the MLE method the selected sectors to compare are sector 2, 6, 9 and 11. Sector 9 and 11 is shown to illustrate apparent good fits. Whereas sector 2 and 6 indicates a poor fit, with the one-year curve showing clear variations from the 10- and 20-year curve. All the sectors are to be found in Appendix F.

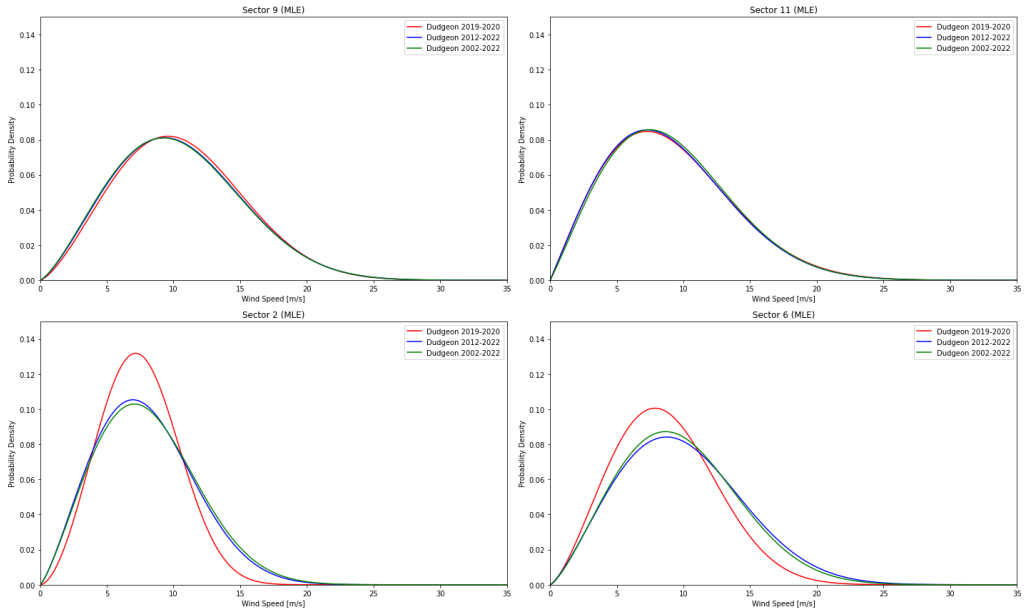

Figure 4.3: Sector 2, 6, 9 and 11 with MLE for different time intervals at Dudgeon.

The p-values for each sector, is presented in Table 4.3. P-values lower than 0.05 are marked with red and indicates a rejecting of the null hypothesis, while green signifies that the hypothesis can be retained. The KS-stat values are higher for the results with one-year data samples compared to the samples with 10-year data, followed by the results from 20-year data with an even lower KS-stat value.

Table 4.3: MLE method KS-stat and p-values for Dudgeon at one-, 10-, and 20 years

Sector	**Dudgeon 2019-2020**		**Dudgeon 2012-2022**		**Dudgeon 2002-2022**	
	KS-stat	**P-value**	**KS-stat**	**P-value**	**KS-stat-stat**	**P-value**
Sector 0	0.0375	0.9539	0.0246	0.2002	0.0196	0.1160
Sector 1	0.0594	0.8587	0.0151	0.8830	0.0162	0.3887
Sector 2	0.0672	0.4859	0.0298	0.0771	0.0251	0.0283
Sector 3	0.1223	0.0270	0.0294	0.1019	0.0335	0.0011
Sector 4	0.0965	0.0457	0.0190	0.4995	0.0212	0.0833
Sector 5	0.0695	0.1895	0.0369	0.0048	0.0265	0.0031
Sector 6	0.0520	0.3951	0.0266	0.0368	0.0302	0.0001
Sector 7	0.0643	0.0700	0.0333	0.0004	0.0283	0.0000
Sector 8	0.0389	0.4178	0.0193	0.0628	0.0170	0.0103
Sector 9	0.0564	0.3094	0.0215	0.1078	0.0144	0.1377
Sector 10	0.0694	0.2675	0.0199	0.3768	0.0166	0.1792
Sector 11	0.0599	0.3862	0.0175	0.6112	0.0153	0.3125

4.1.4 Wind sectors at Dudgeon with L-BFGS-B method

Figure 4.4 presents the Weibull curves at sector 0, 1, 3 and 8 with the L-BFGS-B method at Dudgeon for one-, 10- and 20-year data. For this method the best fit seems to be at sector 0 and 8, unlike sector 1 and 3 where the one-year data differs from the longer periods. The plot of all sectors with L-BFGS-B method are available in Appendix G.

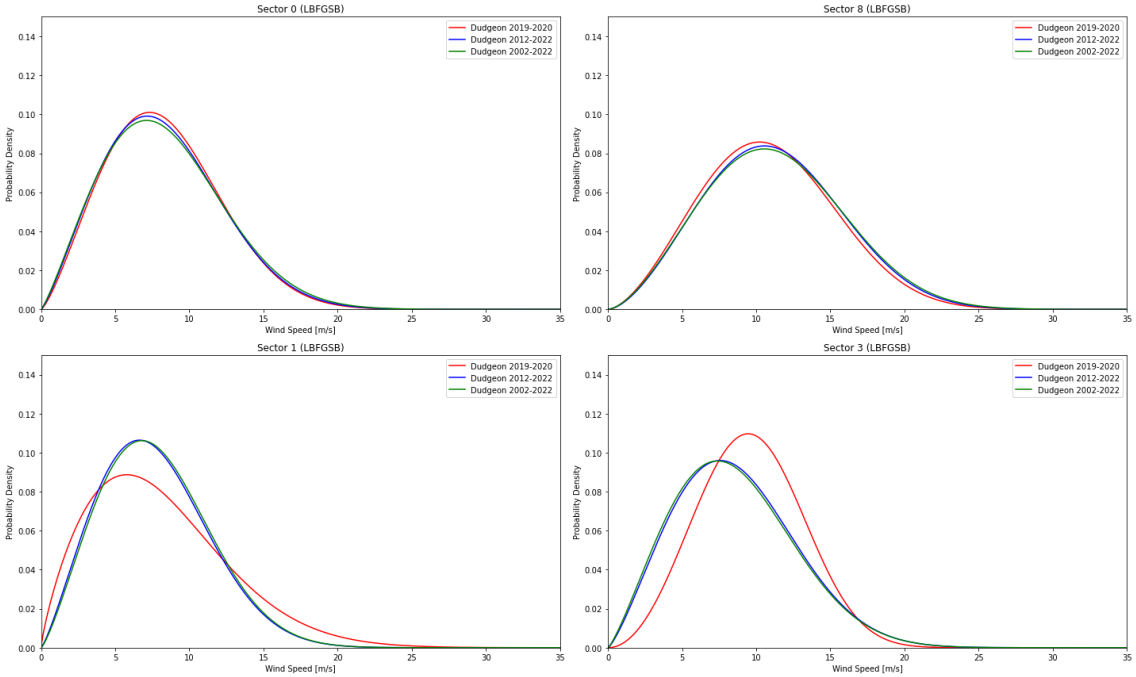

Figure 4.4: Sector 0, 1, 3 and 8 with L-BFGS-B for different time intervals at Dudgeon.

Table 4.4 shows the p-value and KS-stat for Dudgeon with the L-BGFS-B method and are interpreted in the same way as Table 4.3. The KS-stat is higher for the one-year sample and decreases for the consecutive sample sizes.

Table 4.4: L-BFGS-B method KS-stat and P-values for Dudgeon at one-, 10-, and 20 years

Sector	**Dudgeon 2019-2020**		**Dudgeon 2012-2022**		**Dudgeon 2002-2022**	
	KS-stat	**P-value**	**KS-stat**	**P-value**	**KS-stat**	**P-value**
Sector 0	0.0368	0.9605	0.0221	0.3110	0.0165	0.2643
Sector 1	0.0480	0.9697	0.0178	0.7341	0.0178	0.2793
Sector 2	0.0767	0.3240	0.0259	0.1702	0.0214	0.0895
Sector 3	0.1169	0.0390	0.0267	0.1707	0.0295	0.0062
Sector 4	0.0780	0.1683	0.0232	0.3135	0.0229	0.0485
Sector 5	0.0514	0.5357	0.0331	0.0154	0.0294	0.0007
Sector 6	0.0590	0.2513	0.0230	0.1001	0.0266	0.0007
Sector 7	0.0506	0.2487	0.0280	0.0044	0.0226	0.0010
Sector 8	0.0323	0.6542	0.0169	0.1419	0.0148	0.0375
Sector 9	0.0405	0.7171	0.0202	0.1502	0.0169	0.0520
Sector 10	0.0850	0.0988	0.0183	0.4877	0.0127	0.4880
Sector 11	0.0765	0.1393	0.0246	0.2069	0.0153	0.3132

4.2 Dudgeon vs Anholt

The results from the one-year data at Dudgeon and Anholt are given in this section. Both methods MLE and L-BFGS-B are applied to estimate Weibull parameters. The KS test is performed for both cases. The results from the Weibull fitting for each wind sector at the two sites, fail to yield any logical interpretation and is therefore not relevant to include in this section. The results for each sector are given in Appendix H and Appendix I.

4.2.1 Weibull estimation with MLE method

Figure 4.5 presents the Weibull curves for one-year data at Dudgeon and Anholt for the MLE method. Dudgeon is represented with the red line and Anholt with the blue line. It is worth mentioning that the one-year data originates from a different time period for the two sites, explained in Section 3.7. The Weibull parameters and results from the KS test of this total data with MLE at Dudgeon and Anholt are given in Table 4.5.

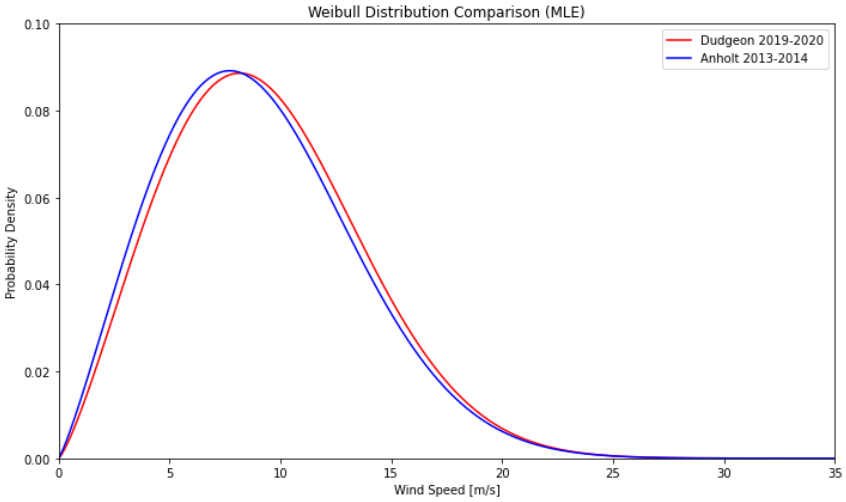

Figure 4.5: Weibull distribution for Dudgeon and Anholt, one-year - MLE.

Table 4.5: MLE Statistics for Anholt and Dudgeon (one-year)

MLE	Anholt, one year	Dudgeon, one year
KS-stat	0.0110	0.0599
P-value	0.0000	0.0117
Shape	2.1846	2.2661
Scale	10.2190	10.5628

In Table 4.6 the KS-stat- and p-values with the MLE method for each sector at Dudgeon and Anholt is presented. The p-values marked green are higher than the significance level at 0.05, previously described in Section 3.6. Unlike the values below 0.05 which is marked with red. It is worth mentioning that even though none of the sectors at Anholt has a p-value higher than 0.05 from the KS test, the KS-stat value is relatively low compared to the Dudgeon case.

Table 4.6: MLE method KS-stat and P-value for Dudgeon and Anholt, one-year

Sector	**Anholt 2013-2014**		**Dudgeon 2019-2020**	
	KS-stat	**P-value**	**KS-stat**	**P-value**
Sector 0	0.0510	0.0000	0.0375	0.9539
Sector 1	0.0326	0.0017	0.0594	0.8587
Sector 2	0.0298	0.0013	0.0672	0.4859
Sector 3	0.0446	0.0000	0.1223	0.0270
Sector 4	0.0498	0.0000	0.0965	0.0457
Sector 5	0.0376	0.0000	0.0695	0.1895
Sector 6	0.0455	0.0000	0.0520	0.3951
Sector 7	0.0556	0.0000	0.0643	0.0700
Sector 8	0.0305	0.0000	0.0389	0.4178
Sector 9	0.0168	0.0348	0.0564	0.3094
Sector 10	0.0305	0.0008	0.0694	0.2675
Sector 11	0.0382	0.0042	0.0599	0.3862

4.2.2 Weibull estimation with L-BFGS-B method

The L-BFGS-B method is applied to estimate a Weibull curve for the one-year data at Dudgeon and Anholt in Figure 4.6. The red and blue represent the Weibull curve for Dudgeon and Anholt respectively. The Weibull fitting for each wind sector is available in Appendix I. Table 4.7 presents the Weibull shape and scale parameters and values from KS test with L-BFGS-B for the entire data sample. Whereas Table 4.8 show KS-test values from each sector.

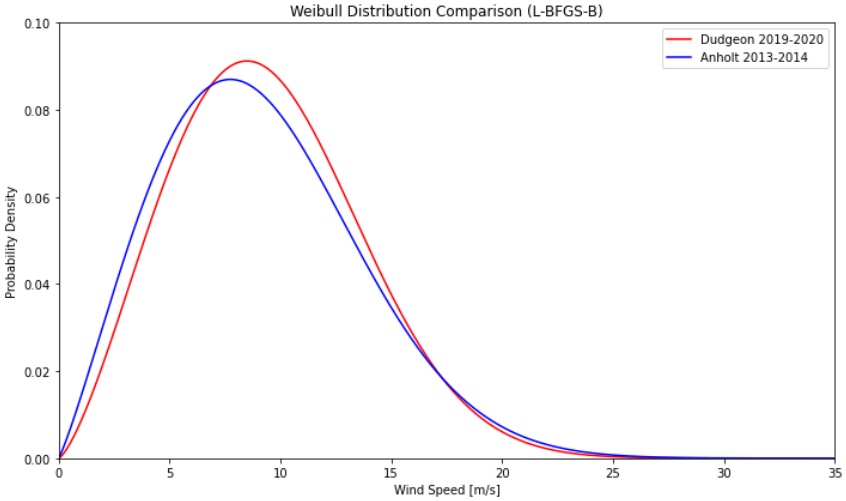

Figure 4.6: Weibull distribution for Dudgeon and Anholt, one-year - L-BFGS-B.

Table 4.7: L-BFGS-B Statistics for Anholt and Dudgeon (one-year)

L-BFGS-B	**Anholt, one year**	**Dudgeon, one year**
KS-stat	0.0136	0.0765
P-value	0.000	0.1393
Shape	2.0060	2.1803
Scale	8.1451	9.4587

Table 4.8: L-BFGS-B method KS-stat and P-values for Dudgeon and Anholt, one-year

Sector	**Anholt 2013-2014**		**Dudgeon 2019-2020**	
	KS-stat	**P-value**	**KS-stat**	**P-value**
Sector 0	0.0400	0.0005	0.0368	0.9605
Sector 1	0.0384	0.0001	0.0480	0.9697
Sector 2	0.0230	0.0257	0.0767	0.3240
Sector 3	0.0372	0.0000	0.1169	0.0390
Sector 4	0.0417	0.0000	0.0780	0.1683
Sector 5	0.0298	0.0024	0.0514	0.5357
Sector 6	0.0352	0.0000	0.0590	0.2513
Sector 7	0.0558	0.0000	0.0506	0.2487
Sector 8	0.0311	0.0000	0.0323	0.6542
Sector 9	0.0191	0.0103	0.0405	0.7171
Sector 10	0.0270	0.0042	0.0850	0.0988
Sector 11	0.0394	0.0028	0.0765	0.1393

4.3 Combination of MLE and L-BFGS-B at Dudgeon

A combination of the wind sectors with the highest p-value was performed to compare whether it would lead to more accurate AEP results from the simulation. The best performing Weibull method from each sector, in regards to the highest p-value was chosen. The Method for each sector and respective shape, scale, KS-stat and p-value are shown in Table 4.9. With this combination, the only sector with a p-value lower than 0.05 is sector 3.

Table 4.9: Results of combining MLE and L-BFGS-B methods

Sector	Shape	Scale	KS-stat	P-value	Method
Sector 0	2.30	9.38	0.037	0.961	L-BFGS-B
Sector 1	1.80	9.07	0.048	0.970	L-BFGS-B
Sector 2	2.80	8.39	0.067	0.486	MLE
Sector 3	3.02	10.79	0.117	0.039	L-BFGS-B
Sector 4	2.76	10.23	0.078	0.168	L-BFGS-B
Sector 5	2.59	10.28	0.051	0.536	L-BFGS-B
Sector 6	2.42	9.79	0.052	0.395	MLE
Sector 7	2.68	11.75	0.051	0.249	L-BFGS-B
Sector 8	2.63	12.27	0.032	0.654	L-BFGS-B
Sector 9	2.27	12.30	0.041	0.717	L-BFGS-B
Sector 10	2.08	10.38	0.069	0.267	MLE
Sector 11	2.02	10.19	0.060	0.386	MLE

4.4 AEP results

The different methods is compared with respect to the AEP given by data from Equinor. Table 4.10 shows the AEP simulation result as a percentage of the provided unfiltered production data, with a one-year data sample.

Table 4.10: AEP with one-year data sample compared to unfiltered production data for Dudgeon 2019-2020

Unfiltered Data	**Time Series**	**Weibull MLE**	**Weibull L-BFGS-B**	**Weibull Combination**
100.0 %	98.4704 %	97.1224 %	101.4713 %	101.9354 %
Deviation	1.5296 %	2.8776 %	1.4713 %	1.9354 %

AEP from the simulations compared to unfiltered production data for each sector at Dudgeon are shown in Table 4.11. The results are based on the one-year sample and are marked with red and green colors to distinguish between underproduction and overproduction respectively. There are some variance between the production from the methods at different sectors. Sectors 0, 1, 2 and 8 are estimating underproduction for all of the methods, with a noticeable difference at sector 0. In addition sector 7, 9 and 10 stands out for time series where it estimates an underproduction. MLE also estimates an underproduction at sector 7, while L-BFGS-B estimates an underproduction at sector 10 and 11 in addition to the sectors mentioned previously.

Table 4.11: AEP for each sector Dudgeon 2019-2020 with one-year data sample

Sector	**Time Series [%]**	**Weibull (MLE) [%]**	**Weibull (L-BFGS-B) [%]**	**Weibull (Combination) [%]**
0	18.9130	58.3388	56.7668	56.3573
1	4.4147	5.3305	0.9059	0.9059
2	5.4068	16.2664	5.5865	16.1479
3	5.3484	10.0699	39.4945	39.1951
4	1.7534	0.6160	18.9121	18.9121
5	14.1507	15.4208	25.7833	25.7833
6	1.2750	8.7685	15.7868	9.0346
7	2.9555	0.3714	4.6460	4.5237
8	1.9792	11.9929	8.7909	8.7909
9	0.0550	8.7947	10.2432	10.2432
10	14.2004	2.2792	7.7021	2.3518
11	7.1209	8.8714	2.8662	8.8714

A comparison of the methods with regard to AEP has also been carried out for the 20-year data sample. The results are presented in Table 4.12 and similar as for the one-year data, the results are in percentage of the provided unfiltered production data from Equinor.

Table 4.12: AEP compared to unfiltered production data for 20-year data sample in Dudgeon

Unfiltered Data	**Time Series**	**Weibull MLE**	**Weibull L-BFGS-B**
100.0 %	101.4400 %	100.8367 %	103.2579 %
Deviation	1.4400 %	0.8367 %	3.2579 %

Table 4.13 shows the compared AEP between simulation and unfiltered production data for each sector for a 20-year data sample from Dudgeon. Numbers marked in red indicates underproduction, while green indicates overproduction. In most cases the relation between the production is the same, except sector 7 where the time series simulation is the only method estimating underproduction.

Table 4.13: Comparison against AEP 20-year - Dudgeon

Sector	**Time Series [%]**	**Weibull (MLE) [%]**	**Weibull (L-BFGS-B) [%]**
0	17.0040 %	54.7919 %	54.1409 %
1	40.1964 %	42.4946 %	44.6288 %
2	28.3856 %	29.2071 %	35.2916 %
3	10.0437 %	13.9688 %	19.6720 %
4	15.8054 %	11.6372 %	7.9294 %
5	12.0409 %	12.3262 %	17.7659 %
6	19.0600 %	22.5825 %	26.3908 %
7	2.5651 %	0.8943 %	3.7233 %
8	8.6691 %	9.4313 %	7.5387 %
9	7.6747 %	7.5178 %	9.1868 %
10	5.0733 %	1.4803 %	1.1286 %
11	1.7200 %	5.1663 %	3.4144 %

5 Discussion

In this section all the estimations, simulations and reflections regarding the Weibull regression methods and AEP results of Anholt and Dudgeon, will be discussed.

5.1 Wind data analysis

A good representation of the wind speed distribution is important in order to achieve accurate simulation result. This section will analyze the overall wind speed representation from the Weibull regression, and determine property differences between MLE and L-BFGS-B method.

From the full sample results for the three different cases at Dudgeon, presented in Figure 4.1 and Figure 4.2 the MLE and L-BFGS-B methods provides slightly different results. The one-year distribution from both simulations visually indicates a higher shape factor in the Weibull function compared to the functions from the 10- and 20-year samples. A reason for this could be that the data 2019-2020 period consists of fewer occurrences with wind speeds above 20 m/s. Figure 4.2 also implies that the L-BFGS-B method favors observations closer to the mode wind speed, rather than outliers. This can be visually determined by the function's steep slope approaching higher wind speeds and high peak around the 9 m/s point. Which is also indicated by the low scale and high shape factor from Table 4.2. This does not seem to be a factor for the 10- and 20-year sample, seeing that a larger data sample naturally evens out the mode wind speed. In comparison, MLE

On the other side, as displayed in Table 3.1 and Table 3.2, the wind data is measured at 100 m and 80 m above sea level respectively for Dudgeon and Anholt. This difference in height might provide wind measurements that should not be compared against each other. Nevertheless, these measurements are the closest to the actual hub height at each site, presented in Table 3.3 and Table 3.4, and was therefore chosen.

5.1.1 Wind sectors

The purpose of evaluating the Weibull regression for each wind direction sector is an effort to validate PyWake's implication of the Bastankhah Porté-Agel model. Since PyWake's simulation model seeks to recreate wind conditions from a sector division, the wind distribution in each sector should be a good representation from the measured wind speeds.

The statistical analysis in Table 4.3 and Table 4.4 of the Dudgeon scenarios indicates that a 10- and 20-year data sample improves the general curve fitting for most sectors, based on the KS-stat. Whereas the p-value indicates a good similarity between the histogram and the Weibull regression for the one-year data samples. When examining the statistical values for the sectors in Anholt, the results in Table 4.6 and Table 4.8 indicates a poor fit from both methods in regards to KS-stat and p-value for all sectors.

The improvement of the KS-stat value for the 10- and 20-year Dudgeon scenarios, shows reasons to mainly correlate with sample size, especially when considering the similarities in the deviation of wind speed and direction from the wind rose diagrams shown in Figure 3.6. On the other hand, the p-values indicates that there is not enough variance between the regression curve and the histogram to reject the null hypothesis for most sectors with smaller data samples.

The correlation between a low p-value from a large sample size, harmonizes well with the results from the Anholt case. Even though the time span for Anholt is only one year, the ten minute intervals provides enough quantitative basis to reject the null-hypothesis for all sectors. On the other hand, it seems like the variation in wind speeds from a one-year sample is not sufficient enough to form a smooth wind speed deviation matching that of a typical Weibull regression, hence explaining the poor KS-stat values.

From this, it could be interpreted that it is not so much the sample size that accumulates a good representation of the wind speed deviation, but rather the time span of the observations. It appears more reasonable to prioritize a representative dispersion of wind speeds indicated by a low KS-stat value and large time span sample, before valuing a good p-value. Additionally it seems appropriate to use three hour intervals for large time span samples, as it represent the wind speed distribution well, and reduces the computational load compared to ten minute intervals. The sites data samples size is therefore variable, which also is the case for the sites wind direction, which can be seen from the wind roses.

From the two sites one-year wind rose in Section 3.5.2, the majority of the wind is coming from southwest in both cases. Nevertheless the variance in wind direction is greater at Anholt than for Dudgeon. At Anholt the wind occurs slightly more directly from west (270°), and also a comprehensive part from southwest (180° - 250°). Even though the shortest distance to shore for Anholt is towards southwest, and directly towards west gives a greater distance to shore, there is no extreme difference in wind measurements. But it is worth mentioning that the amount of wind speeds greater than 15 m/s happens more often directly from west and south at Anholt. Based on this, it is possible that Anholt experience lower wind speeds from the directions closer to shore. This concur well with mentioned theory in Section 2.3, as it in general are lower wind speeds closer to shore. Nevertheless, the wind characteristics vary with local conditions.

When looking at the wind rose for Dudgeon, the wind is more concentrated against southwest (225°). This direction is also where the highest wind speeds for Dudgeon are experienced. From Figure 4.5 and Figure 4.6 the Weibull at Dudgeon is skewed to the right both for MLE and L-BFGS-B methods. The results are not enough evidence to make a conclusion whether the distance from shore have a big impact on the wind data and production, but it seems to be several occurrences of higher wind speeds at Dudgeon compared to Anholt, which may result in a higher energy production at this site. Though it is difficult to state if the distance from shore have a big affection on the results in this case.

5.2 AEP analysis

All the analysis in this section is refereed to the Dudgeon site and based on the comparison between PyWake simulations and the acquired production data from Equinor. The result section indicates that the basis for validating the use of Weibull pdf's to approximate the wind speed dispersion is different for the total AEP and the AEP from each wind direction sector.

5.2.1 Total AEP

The AEP results in the report are used as a means of action in order to validate the use of Weibull regression, as a representative wind speed dispersion approximation. From the AEP comparisons in Table 4.11, it is notably the L-BFGS-B method that gives the most accurate simulation result, when simulating with Weibull functions constructed from a one-year data sample. Table 4.13 shows the results from the simulations where the curves are constructed from a 20-year sample size. For this time span, the MLE method proves to be the overall most accurate simulation method.

When considering the importance of sample size, the AEP results regarding MLE seems to support the claim from the wind sector analysis in Section 5.1.1, that a low KS-stat value should be valued above acceptable p-values for more precise simulations. Nevertheless it is an interesting mention that the simulations from the one-year sample, deviate with almost 2.9 % for MLE, given that only two sectors are rejected from the null hypothesis. According to theory, a p-value over 0.05 should indicate a degree of similarity between two samples, and hence reason to believe that the wind speed distribution is well represented, even though it is not the case of MLE. Interestingly, L-BFGS-B deviates with 3.26 % for the 20-year data sample, and is the least accurate result from all scenarios, whereas MLE only deviates with 0.8367 %. Unlike MLE, L-BFGS-B seems to lean in the favor of a high p-value above low KS-stat, being that the method performed the best for a smaller sample size with a deviation of 1.47 %. The effort to combine the two methods for the one-year data resulted in an AEP deviation of 1.94 %. After the considerations just mentioned, it is difficult to conclude any optimal combination from the two methods as a definite best fit. Both methods shows characteristics beneficial for different scenarios. Another simulation with a combination of curves selected by the lowest KS-stat value would give a better insight to the theory.

The use of Weibull regression to approximate the total AEP appears reasonable, especially for the MLE method with a 20-year time period. It is worth mentioning that the total deviation of 0.8367 % in AEP, is an substantial amount of energy considering Dudgeon's installed capacity of 402 MW, but for this report, it is the best performing result. Notably, the results indicate that it is more appropriate to utilize the L-BFGS-B method instead of MLE for smaller sample sizes. In order to draw further conclusions in regard to good AEP estimations, more production data seems necessary.

5.2.2 AEP in each sector

Further analysis showed that even though the total AEP from the simulation result correlated well with the actual production data, the same can not be determined for each wind direction sector individually. PyWake's Bastankhah Porté-Agel model uses a normalized probability of occurrence vector from the wind direction KDE regression, in order to simulate the ratio of production dedicated to each sector. This results in the sector AEP being a product of both the KDE regression and Weibull, essentially adding another degree of uncertainty.

Table 3.7, show that the probability of occurrence is increasing with every sector incremental, and peaks at sector 8, before decreasing. The unfiltered production also follows this trend with the exception of sector 0. From Table 4.11 and 4.13 it is clear that the AEP in sector 0 is greatly underestimated by all simulations for both sample size cases. The tables show altercations between over-and underestimating for both methods.

In Table 3.8 the wind direction sample size from the 2019-2020 data seems to correlate reasonably well with the production distribution from Equinor. By analyzing the KDE regression, it is clear that the method cuts out the peaks for sector 0 in favor of a smoother curve fitting. Hence underestimating the actual probability of instances with wind directions between 345° and 15°. Another point is that all the sector AEP results for the 20-year data sample is compared to the one-year production data, and as seen from the 20-year sample distribution in Table 3.8, the wind direction conditions from 2019-2020 does not correlate with the mean distribution over a longer time period. Considering the poor estimation for sector 0 from the KDE, it makes sense that it effects the AEP accuracy for the other sectors simulation. From the one-year production comparison, Table 4.11 shows that the two Weibull methods have clear production deviations for some of the sectors. The 20-year data sample from Table 4.13 shows more similarities between the two methods. Both methods show overestimation and underestimations for the same sectors, where L-BFGS-B generally overestimates more than MLE, and MLE underestimates more than L-BFGS-B. It is difficult to draw any conclusions regarding Weibull fits from the KS-stat or p-values due to the inaccuracy from the KDE.

The accuracy from the sector simulations seems to mostly rely on the twelve wind direction probability parameters from the KDE. The previous assumption of MLE being the most valid method for large data samples is not contradicted from the sector analysis, but the analysis suffers from a misrepresentation of the wind sector divisions. The application of a KDE distribution leads to more uncertainties, and a normalized distribution from the sample occurrences seem more appropriate.

5.3 Time Series Evaluation

The time series simulation model in PyWake computes the entire time series vector from the wind direction and wind speed parameters based on the users input data. In this case the 2019-2020 and 2002-2022 wind data sample from Nora10. Being that the simulation does not use any approximation tools it should be expected to be a good representation for the AEP. The results from Section 4.4 show that the simulations perform second best in regard to deviation, for both sample size cases. The 20-year case has the best result, with a deviation of 1.44 %. From the AEP data for each sector, the time series simulation can be seen to follow the same trend as MLE and L-BFGS-B in regards to alternating between over and underestimations.

The AEP in the 20-year data sample case indicates a poor representation for most wind sectors. This correlates well with the difference in the spread of datapoints from the production data and the Nora10 data seen from Table 3.8. From the one-year data sample, the sector AEP seems to be represented well with the exception of sector 0, 5 and 10 with a deviation of 18.9 %, 14.2 % and 14.2 % respectively. Sector 0 and 10 are also poorly represented by the Weibull methods, but can be partially explained from the KDE regression. The results from the time series sectors indicates that the deviation in AEP is affected by other factors, being that the simulation is independent from the KDE.

This report investigated the time series simulation with the expectation of it being the most accurate simulation model with the downside of a time demanding computational time. As an additional mention in regards to simulation time, none of the simulations suffered from relatively long processing times from PyWake's script. As to the relevance of computational time, the topic may seem more relevant for more advanced simulation tools, but not PyWake. Nevertheless, based on the results from the report, simulations with the

Weibull model should be prioritized. It is difficult to conclude with a definite reason for the inaccuracy of the time series simulation, and is something that should be examined further.

5.4 Further work

As a general mention to the conclusions drawn from the observations in this report , it must be pointed out that several key factors had to be excluded from the study. As mentioned in Section 3.5, small adjustments in the wake expansion factor k^* can have a large impact on the simulation result. Nevertheless, the wake expansion factor constant from PyWake, did indeed provide a relatively close approximation to the actual AEP, and gave a good basis for evaluating the Bastankhah Porté-Agel Weibull simulation. That being said, a more accurate approach to determine the factor k^*, would improve the quality of the results.

The turbulence intensity is also not considered for any of the simulation, and was a simplification in order to limit the extent of the study. The PyWake module contain several models that could include the TI parameter, but seeing as the k^* factor is a product of TI, it was deemed sufficient to choose a model that exclude the parameter, in favor of a constant wake expansion factor. Regardless, the change in wind turbulence is an important parameter needed in order to better simulate the actual physiological behavior of wind. It is important to emphasize that further studies should strive to address the influence from TI.

As discussed, it would be interesting to investigate if a combination of the methods MLE and L-BFGS-B, with focus on the sectors with lowest KS-stat values instead of p-values could lead to more accurate estimation regarding AEP. Also as mentioned in Section 2.5.1, there are several other viable Weibull regression methods that could be interesting to investigate. Especially in regard to the Weibull curves for the twelve wind sectors, and difference in sample size.

A further realization from the study, in regards to power production, is the relationship between the wind turbine power curve and the Weibull regression of the wind speed histogram, given that there is an non-linear correlation between them. As an example, there are instance where the Weibull regression underestimates the occurrence of wind speeds at 20 m/s in favor of a smoother curve in the area of lower wind speeds. This balances the numerical values in the wind speed histogram, but does not give a correct correlation to the actual power production, given that the production from a wind speed of 13 m/s is exponentially higher than 5 m/s. Attempting to implementing a Weibull fit for a wind speed histogram as a function of power density, would be an interesting approach that could possibly lead to more accurate simulation results.

To further validate the Weibull distribution as a reliable estimation for AEP, future research should be done with more cases with other wind farm locations. It is possible for the distributions in other locations further offshore and closer to shore would give some different results according to the Weibull distributions. It would also be beneficial to look at locations with similar wind turbine types.

6 Conclusion

The goal of this thesis was to investigate whether Weibull estimations is a reasonable approach for assessing an offshore wind farm's wind speed conditions and AEP. The Weibull estimation for wind speed seems to make a good representation to the original wind data in both cases. A key finding was that the MLE method proved to be the most accurate optimization algorithm for the 20-year data samples, and L-BFGS-B for the one-year sample with deviations of 0.8376 % and 1.47 % respectively. The difference in how well the MLE and L-BFGS-B method performed, indicates the importance of the sample size for simulating a precise prognosis of AEP. Accurate and long term wind conditions data are valuable for improving the energy production estimations for the offshore industry.

Even though the overall production prediction were reliable, the AEP from each individual wind sector did not have a clear correspondence to the 2019-2020 production data. Analysis indicated that the representation of wind direction from the KDE regression was a partial reason for the imprecise deviation in AEP. Nevertheless, from the research it is valid to assume that sectors with more occurring wind speed should prioritize MLE method, and the same can be said for the L-BFGS-B method for the less occurring sectors.

Since offshore wind farms are intended to remain operational for several years. Weibull application should be based on long time span data samples, as concluded from the 20 year sample case in this report. For further development and optimization of offshore wind farms, a closer look at different variations of combination of methods will be beneficial. By doing so, the methods strength could possibly create a hybrid model more accurate regarding AEP estimation. This can be done for multiple methods in order to find the most optimal alternative.

Bibliography

[1] R. Wiser et al. *Wind Energy. In IPCC Special Report on Renewable Energy Sources and Climate Change Mitigation, [O. Edenhofer, R. Pichs-Madruga, Y. Sokona, K. Seyboth, P. Matschoss, S. Kadner, T. Zwickel, P. Eickemeier, G. Hansen, S. Schlömer, C. von Stechow (eds)]*, tech. rep. Cambridge University Press, Cambridge, United Kingdom and New York, NY, USA., 2011. URL: https://www.ipcc.ch/site/assets/uploads/2018/03/Chapter-7-Wind-Energy-1.pdf.

[2] Natalia Moskalenko, Krzysztof Rudion, and Antje Orths. "Study of wake effects for offshore wind farm planning". In: *2010 Modern Electric Power Systems*. IEEE. (2010), pp. 1–7. URL: https://ieeexplore.ieee.org/stamp/stamp.jsp?tp=&arnumber=6007187.

[3] Marian Felix Polster. "Comprehensive comparison of analytical wind turbine wake models with wind tunnel measurements and wake model application on performance modelling of a downstream turbine". MA thesis. NTNU, (2017). URL: https://ntnuopen.ntnu.no/ntnu-xmlui/bitstream/handle/11250/2454926/17955_FULLTEXT.pdf?sequence=1&isAllowed=y.

[4] L. J. Vermeer, J. N. Sørensen, and A. Crespo. *Wind turbine wake aerodynamics*. Tech. rep. Progress in Aerospace Sciences, 2003. URL: https://www.sciencedirect.com/science/article/pii/S0376042103000782?ref=pdf_download&fr=RR-2&rr=86dfcef61c695696.

[5] R. J. Barthelmie et al. *Modelling and Measuring Flow and Wind Turbine Wakes in Large Wind Farms Offshore*. Tech. rep. Wiley Interscience, June 2009. URL: https://onlinelibrary.wiley.com/doi/epdf/10.1002/we.348.

[6] John Sondre Sikkeland. "Power prediction and wake losses in offshore wind farms with the dynamic wake meandering model". MA thesis. Norwegian University of Life Sciences, Ås, (2020). URL: https://nmbu.brage.unit.no/nmbu-xmlui/bitstream/handle/11250/2725555/Sikkeland_2020.pdf?sequence=2&isAllowed=y.

[7] Majid Bastankhah and Fernando Porté-Agel. "A new analytical model for wind-turbine wakes". In: *Renewable Energy* 70 (2014), pp. 116–123. ISSN: 0960-1481. DOI: https://doi.org/10.1016/j.renene.2014.01.002. URL: https://www.sciencedirect.com/science/article/pii/S0960148114000317.

[8] Leif Rasmussen et al. *Wind Farm Wake: The Horns Rev Photo Case*. Tech. rep. DTU, Danish Meteorological Institute, DONG Energy, May 2013. URL: https://www.mdpi.com/1996-1073/6/2/696.

[9] Paul van der Laan Mads M. Pedersen Alexander Meyer Forsting et al. "PyWake 2.5.0: An open-source wind farm simulation tool". In: (Feb. 2023). URL: https://gitlab.windenergy.dtu.dk/TOPFARM/PyWake.

[10] N. O. Jensen. *A Note on Wind Generator Interaction*. Tech. rep. Risø National Laboratory, 1983. URL: https://backend.orbit.dtu.dk/ws/portalfiles/portal/55857682/ris_m_2411.pdf.

[11] S.-L. Tai et al. "Validation of turbulence intensity as simulated by the Weather Research and Forecasting model off the US northeast coast". In: *Wind Energy Science* 8.3 (2023), pp. 433–448. DOI: 10.5194/wes-8-433-2023. URL: https://wes.copernicus.org/articles/8/433/2023/.

[12] R. Barthelmie and Sara Pryor. "Automated wind turbine wake characterization in complex terrain". In: *Atmospheric Measurement Techniques* 12 (June (2019)), pp. 3463–3484. URL: https://amt.copernicus.org/articles/12/3463/2019/amt-12-3463-2019.pdf.

[13] Mingwei Ge et al. "A two-dimensional model based on the expansion of physical wake boundary for wind-turbine wakes". In: *Applied Energy* 233-234 (2019), pp. 975–984. ISSN: 0306-2619. DOI: https://doi.org/10.1016/j.apenergy.2018.10.110. URL: https://www.sciencedirect.com/science/article/pii/S0306261918316817.

[14] Luca Lanzilao and Johan Meyers. "A new wake-merging method for wind-farm power prediction in the presence of heterogeneous background velocity fields". In: *Wind Energy* 25 (July 2021). DOI: 10.1002/we.2669.

[15] Paul van der Laan Mads M. Pedersen Alexander Meyer Forsting et al. "PyWake 2.5.0: Wake Model Description for Optimization Only Case Study". In: *GitHub* (Feb. 2019). URL: https://github.com/byuflowlab/iea37-wflo-casestudies/blob/master/cs1-2/iea37-wakemodel.pdf (visited on 05/08/2024).

[16] J. P. Kofoed and M. Folley. "Chapter 13 - Determining Mean Annual Energy Production". In: *Numerical Modelling of Wave Energy Converters*. Ed. by Matt Folley. Academic Press, Jan. 2016, pp. 253–266. ISBN: 978-0-12-803210-7. DOI: 10.1016/B978-0-12-803210-7.00013-X. URL: https://www.sciencedirect.com/science/article/pii/B978012803210700013X.

[17] T. Wizelius. "2.13 - Design and Implementation of a Wind Power Project". In: *Comprehensive Renewable Energy*. Ed. by Ali Sayigh. Oxford: Elsevier, Jan. 2012, pp. 391–430. ISBN: 978-0-08-087873-7. DOI: 10.1016/B978-0-08-087872-0.00215-8. URL: https://www.sciencedirect.com/science/article/pii/B9780080878720002158 (visited on 04/21/2024).

[18] Lars Frøyd and revised by Tania Bracchi Svein Kjetil Haugset. *Compendium on Blade Design for HAWT using BEM*. 2022. (Visited on 08/05/2024).

[19] Tableau. *Time Series Analysis: Definition, Types, Techniques, and When It's Used*. URL: https://www.tableau.com/learn/articles/time-series-forecasting (visited on 04/26/2024).

[20] Florin Onea and Eugen Rusu. "An Assessment of Wind Energy Potential in the Caspian Sea". In: 12 (July 2019), p. 2525. DOI: 10.3390/en12132525.

[21] Abdulbaset El-bshah et al. "Resource Assessment of Wind Energy Potential of Mokha in Yemen with Weibull Speed". In: *Computers, Materials and Continua* 69 (Jan. 2021), pp. 1123–1140. DOI: 10.32604/cmc.2021.018427.

[22] Robert Sheldon. *What is a histogram? | Definition from TechTarget*. en. June 2023. URL: https://www.techtarget.com/searchsoftwarequality/definition/histogram (visited on 04/27/2024).

[23] NTNU. *Wind data analysis | Module 6 : Wind characteristics and resource assessment | Wind Energy and Design of a Wind Turbine (TEP4175 - FENT2321) | DIGIT - Platform for online courses*. URL: https://apps.digit.ntnu.no/learning/course/course-v1:NTNU+IE-IVP+2023_AUG/block-v1:NTNU+IE-IVP+2023_AUG+type@sequential+block@ef1bf0af1bdc4e5d924664a783247334/block-v1:NTNU+IE-IVP+2023_AUG+type@vertical+block@9cc4cc1195d244789ae0babef33a2fa0 (visited on 04/29/2024).

[24] Ahmet Pekgor Asir Genc Murat Erisoglu et al. "Estimation of Wind Power Potential Using Weibull Distribution". In: *Energy Sources* 27.9 (2005). Publisher: Taylor & Francis _eprint: https://doi.org/10.1080/00908310490450647, pp. 809–822. DOI: 10.1080/00908310490450647. URL: https://doi.org/10.1080/00908310490450647.

[25] Salahaddin A Ahmed. "Comparative study of four methods for estimating Weibull parameters for Halabja, Iraq". In: (2013). URL: https://citeseerx.ist.psu.edu/document?repid=rep1&type=pdf&doi=c0b22f8ce58f84bb438a757258127d914fdc27be.

[26] Paritosh Bhattacharya and Rakhi Bhattacharjee. "A Study on Weibull Distribution for Estimating the Parameters". In: *Wind Engineering* 33.5 (2009). _eprint: https://doi.org/10.1260/030952409790291163, pp. 469–476. DOI: 10.1260/030952409790291163. URL: https://doi.org/10.1260/030952409790291163.

[27] Harsh Patidar et al. "Comparative study of offshore wind energy potential assessment using different Weibull parameters estimation methods". en. In: *Environmental Science and Pollution Research* 29.30 (June 2022), pp. 46341–46356. ISSN: 1614-7499. DOI: 10.1007/s11356-022-19109-x. URL: https://doi.org/10.1007/s11356-022-19109-x (visited on 05/01/2024).

[28] Carsten Croonenbroeck and David Hennecke. "A comparison of optimizers in a unified standard for optimization on wind farm layout optimization". In: *Energy* 216 (Feb. 2021), p. 119244. ISSN: 0360-5442. DOI: 10.1016/j.energy.2020.119244. URL: https://www.sciencedirect.com/science/article/pii/S0360544220323513 (visited on 05/04/2024).

[29] A. Ayik et al. "Preliminary wind resource assessment in South Sudan using reanalysis data and statistical methods". In: *Renewable and Sustainable Energy Reviews* 138 (Mar. 2021), p. 110621. ISSN: 1364-0321. DOI: 10.1016/j.rser.2020.110621. URL: https://www.sciencedirect.com/science/article/pii/S1364032120309059.

[30] José Antonio Guarienti et al. "Performance analysis of numerical methods for determining Weibull distribution parameters applied to wind speed in Mato Grosso do Sul, Brazil". In: *Sustainable Energy Technologies and Assessments* 42 (Dec. 2020), p. 100854. ISSN: 2213-1388. DOI: 10.1016/j.seta.2020.100854. URL: https://www.sciencedirect.com/science/article/pii/S2213138820312819 (visited on 05/09/2024).

[31] *Estimation of Wind Power Potential Using Weibull Distribution*. en. DOI: 10.1080/00908310490450647. URL: https://www.tandfonline.com/doi/epdf/10.1080/00908310490450647?needAccess=true (visited on 05/02/2024).

[32] *Improving the FLORIS wind plant model for compatibility with gradient-based optimization*. en. DOI: 10.1177/0309524X17722000. URL: https://journals.sagepub.com/doi/epub/10.1177/0309524X17722000 (visited on 05/02/2024).

[33] Rafael Valotta Rodrigues et al. "Speeding up large-wind-farm layout optimization using gradients, parallelization, and a heuristic algorithm for the initial layout". In: *Wind Energy Science* 9.2 (Feb. 2024). Publisher: Copernicus GmbH, pp. 321–341. ISSN: 2366-7443. DOI: 10.5194/wes-9-321-2024. URL: https://wes.copernicus.org/articles/9/321/2024/.

[34] Mohammad Mushir Riaz and Badarul Hasan Khan. *IEEE Xplore Full-Text PDF:* URL: https://ieeexplore.ieee.org/stamp/stamp.jsp?tp=&arnumber=8980167 (visited on 05/01/2024).

[35] Z. R. Shu, Q. S. Li, and P. W. Chan. "Investigation of offshore wind energy potential in Hong Kong based on Weibull distribution function". In: *Applied Energy* 156 (Oct. 2015), pp. 362–373. ISSN: 0306-2619. DOI: 10.1016/j.apenergy.2015.07.027. URL: https://www.sciencedirect.com/science/article/pii/S0306261915008569 (visited on 05/01/2024).

[36] In Jae Myung. "Tutorial on maximum likelihood estimation". In: *Journal of Mathematical Psychology* 47.1 (Feb. 2003), pp. 90–100. ISSN: 0022-2496. DOI: 10.1016/S0022-2496(02)00028-7. URL: https://www.sciencedirect.com/science/article/pii/S0022249602000287 (visited on 04/28/2024).

[37] Muhammad Akram and Aziz Hayat. "Comparison of Estimators of the Weibull Distribution". en. In: *Journal of Statistical Theory and Practice* 8.2 (June 2014), pp. 238–259. ISSN: 1559-8616. DOI: 10.1080/15598608.2014.847771. URL: https://doi.org/10.1080/15598608.2014.847771 (visited on 05/21/2024).

[38] Zhibin Tan. "A new approach to MLE of Weibull distribution with interval data". In: *Reliability Engineering & System Safety* 94.2 (Feb. 2009), pp. 394–403. ISSN: 0951-8320. DOI: 10.1016/j.ress.2008.01.010. URL: https://www.sciencedirect.com/science/article/pii/S0951832008001300 (visited on 05/21/2024).

[39] Scott A Czepiel. "Maximum Likelihood Estimation of Logistic Regression Models: Theory and Implementation". In: (). URL: https://saedsayad.com/docs/mlelr.pdf.

[40] R. H. Byrd, L. Peihuang, and J. Nocedal. *A limited-memory algorithm for bound-constrained optimization*. English. Report. Number: MCS–P404-1293 Publisher: Argonne National Laboratory. Mar. 1996. DOI: 10.2172/204262. URL: https://digital.library.unt.edu/ark:/67531/metadc666315/ (visited on 05/02/2024).

[41] Ciyou Zhu et al. "Algorithm 778: L-BFGS-B: Fortran subroutines for large-scale bound-constrained optimization". en. In: *ACM Transactions on Mathematical Software* 23.4 (Dec. 1997), pp. 550–560. ISSN: 0098-3500, 1557-7295. DOI: 10.1145/279232.279236. URL: https://dl.acm.org/doi/10.1145/279232.279236 (visited on 05/04/2024).

[42] Hayriye Esra Akyuz and Hamza Gamgam. "Statistical Analysis of Wind Speed Data with Weibull, Lognormal and Gamma Distributions". en. In: *Cumhuriyet Science Journal* (Dec. 2017), pp. 68–76. ISSN: 2587-2680. DOI: 10.17776/csj.358773. URL: https://dergipark.org.tr/en/doi/10.17776/csj.358773 (visited on 05/09/2024).

[43] Chinmaya Kar and A. R. Mohanty. "Application of KS test in ball bearing fault diagnosis". In: *Journal of Sound and Vibration* 269.1 (Jan. 2004), pp. 439–454. ISSN: 0022-460X. DOI: 10.1016/S0022-460X(03)00380-8. URL: https://www.sciencedirect.com/science/article/pii/S0022460X03003808 (visited on 05/07/2024).

[44] Pauli Virtanen et al. "SciPy 1.0: Fundamental Algorithms for Scientific Computing in Python". In: *Nature Methods* 17 (2020), pp. 261–272. DOI: 10.1038/s41592-019-0686-2. URL: https://docs.scipy.org/doc/scipy/reference/generated/scipy.stats.kstest.html.

[45] Kyriaki Corinna Datsiou and Mauro Overend. "Weibull parameter estimation and goodness-of-fit for glass strength data". In: *Structural Safety* 73 (July 2018), pp. 29–41. ISSN: 0167-4730. DOI: 10.1016/j.strusafe.2018.02.002. URL: https://www.sciencedirect.com/science/article/pii/S0167473016301904 (visited on 05/09/2024).

[46] Hubert W. Lilliefors. "On the Kolmogorov-Smirnov Test for Normality with Mean and Variance Unknown". en. In: *Journal of the American Statistical Association* 62.318 (June 1967), pp. 399–402. ISSN: 0162-1459, 1537-274X. DOI: 10.1080/01621459.1967.10482916. URL: http://www.tandfonline.com/doi/abs/10.1080/01621459.1967.10482916 (visited on 05/14/2024).

[47] Ørsted. *Offshore wind data*. URL: https://orsted.com/en/what-we-do/renewable-energy-solutions/offshore-wind/offshore-wind-data (visited on 05/02/2024).

[48] M. Paul van der Laan et al. "Challenges in simulating coastal effects on an offshore wind farm". In: *Journal of Physics: Conference Series* 854 (May 2017), p. 012046. DOI: 10.1088/1742-6596/854/1/012046.

[49] Dudgeon Offshore Wind Farm. *Dudgeon Offshore Wind Farm | Index*. URL: https://dudgeonoffshorewind.co.uk/index.php (visited on 04/25/2024).

[50] Equinor. *Sniktitt bak kulissene: Dogger Bank havvindpark tar form*. no. URL: https://www.equinor.com/no/magasin/sniktitt-pa-byggingen-av-dogger-bank-havvindpark (visited on 04/04/2024).

[51] Dudgeon Offshore Wind Farm. *Dudgeon Offshore Wind Farm | Turbines*. URL: https://dudgeonoffshorewind.co.uk/construction/turbines (visited on 04/25/2024).

[52] WindAtlas. *Windatlas - Windfarm*. URL: http://windatlas.xyz/farm/?name=Dudgeon (visited on 04/25/2024).

[53] Dudgeon Offshore Wind Farm. *Dudgeon Offshore Wind Farm | Facts & Figures*. URL: https://dudgeonoffshorewind.co.uk/construction/facts-and-figures (visited on 04/04/2024).

[54] Power Technology. *Dudgeon Offshore Wind Farm*. en-US. Jan. 2018. URL: https://www.power-technology.com/projects/dudgeon-offshore-wind-farm/ (visited on 04/25/2024).

[55] Equinor. *Dudgeon Offshore Wind Farm contracts to Siemens plc - equinor.com*. en. Jan. 2014. URL: https://www.equinor.com/news/archive/2014/01/14/13JanDudgeon (visited on 04/25/2024).

[56] Dudgeon Offshore Wind Farm. *Dudgeon Offshore Wind Farm*. URL: https://dudgeonoffshorewind.co.uk/ (visited on 02/09/2024).

[57] Ørsted. "Orsted_A4_brochure_Anholt_04_UK.indd". In: (). URL: https://orsted.com/-/media/www/docs/corp/com/our-business/wind-power/wind-farm-project-summary/anholt_uk_2018.ashx?la=en&hash=7707175e111c65a4aefc353291091ee4.

[58] Ørsted. *Offshore wind energy*. en. URL: https://orsted.com/en/what-we-do/renewable-energy-solutions/offshore-wind (visited on 04/25/2024).

Appendix

A Appendix - Anholt Layout

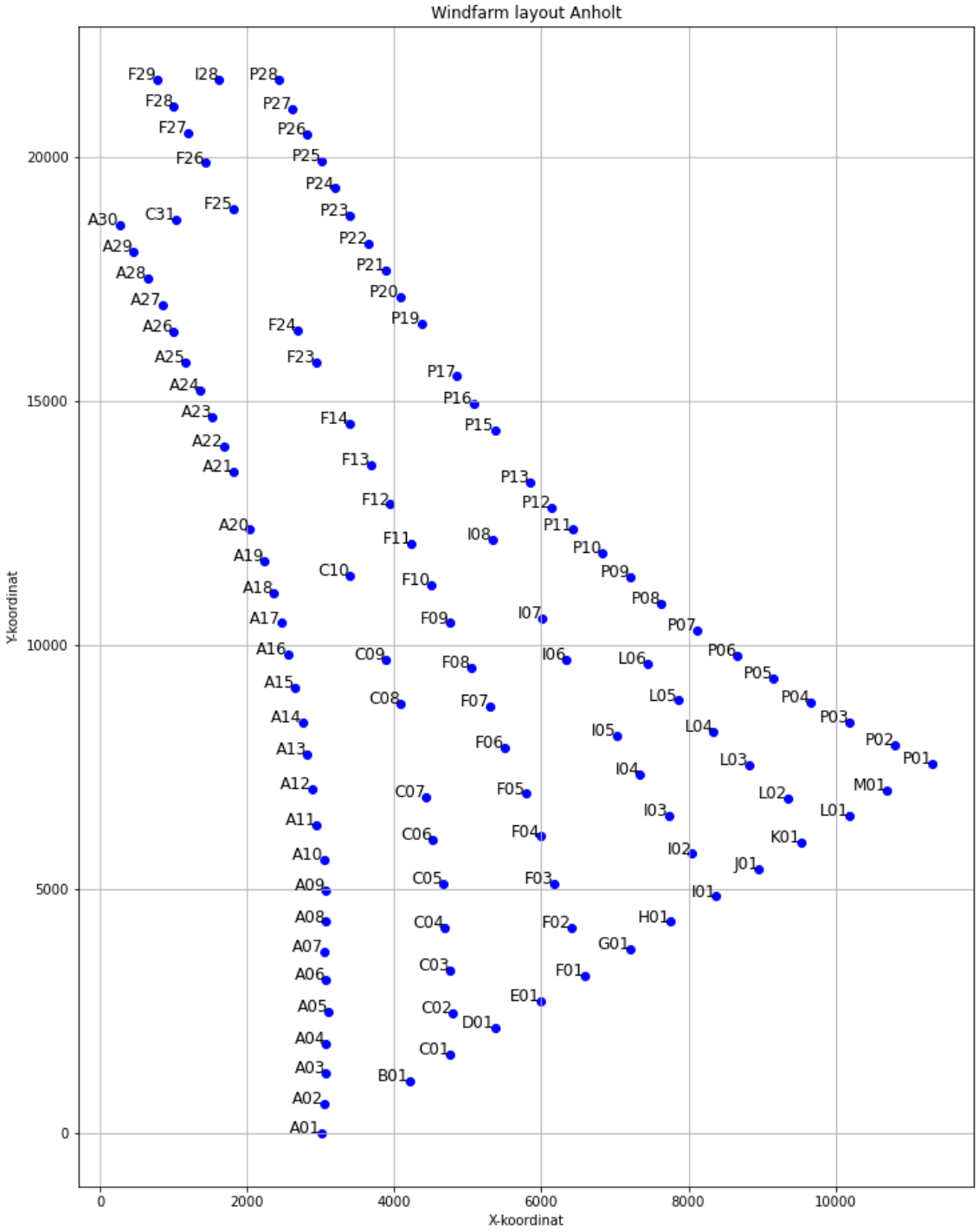

B Appendix - Wind sectors at Dudgeon and Anholt with MLE method

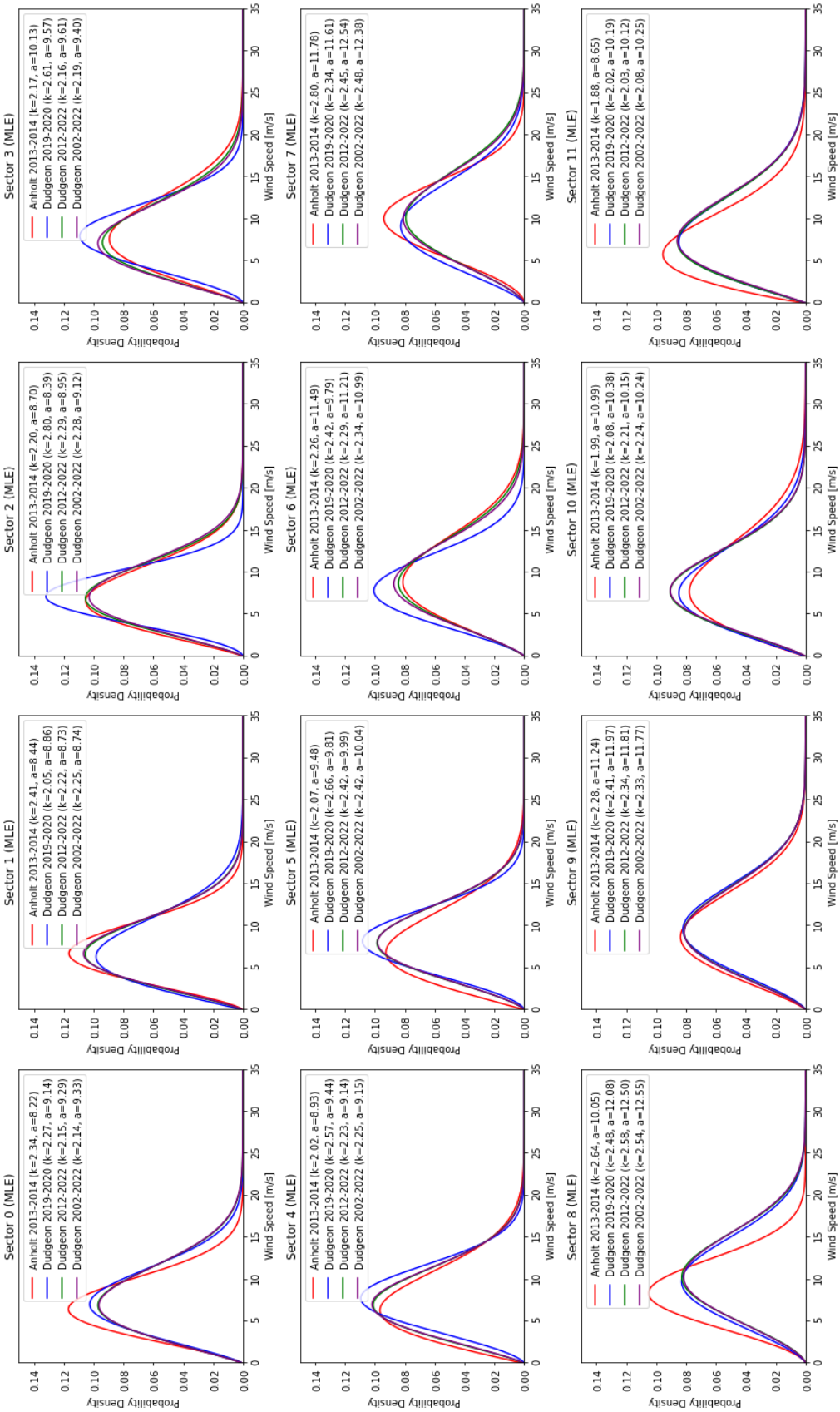

C Appendix - Wind sectors at Dudgeon and Anholt with L-BFGS-B method

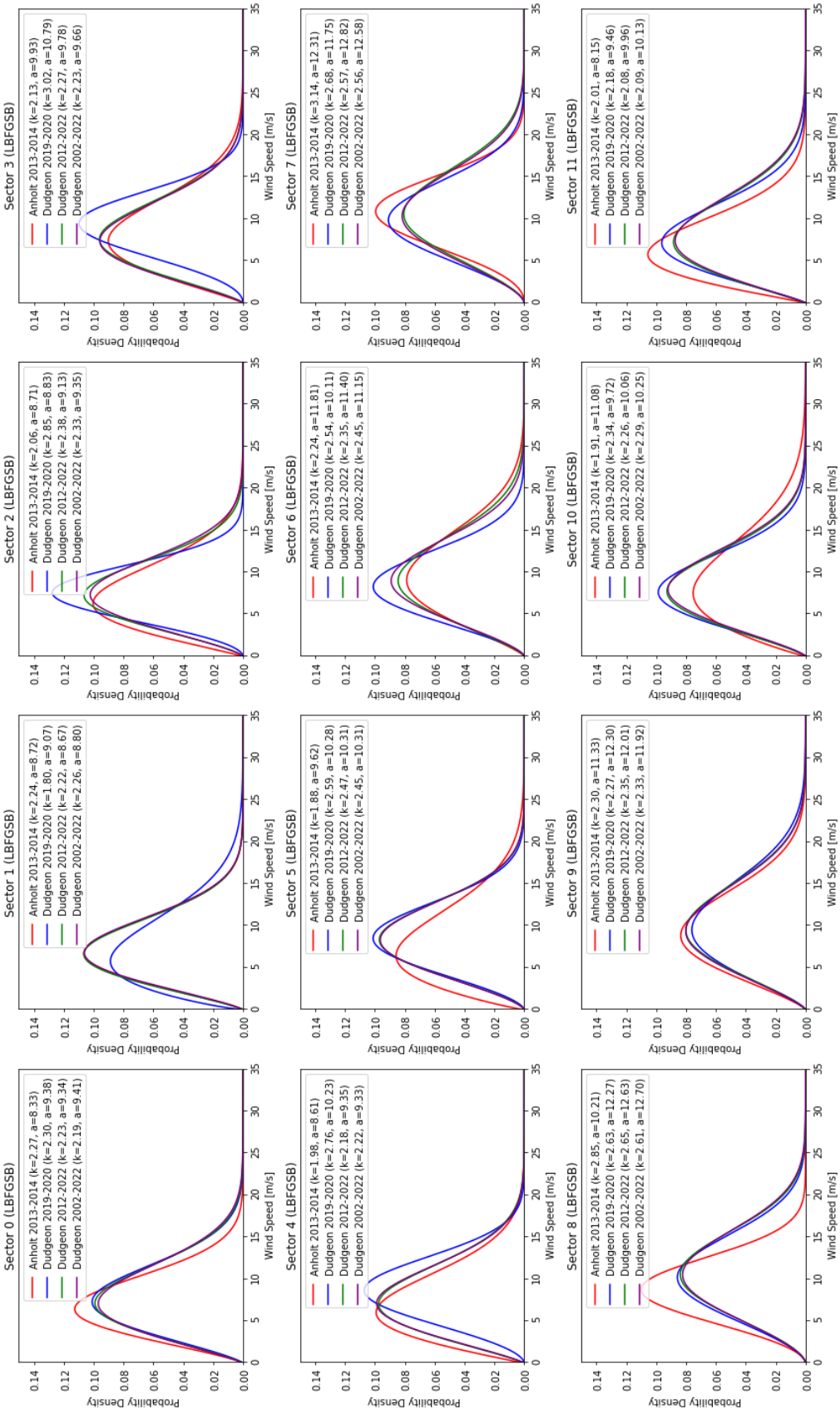

D Appendix - Weibull parameters for Dudgeon and Anholt with MLE and L-BFGS-B method

MLE	Shape	Shape	Shape	Shape	Scale	Scale	Scale	Scale
	Anholt 2013-2014	Dudgeon 2019-2020	Dudgeon 2012-2022	Dudgeon 2002-2022	Anholt 2013-2014	Dudgeon 2019-2020	Dudgeon 2012-2022	Dudgeon 2002-2022
Sector 0	2.34333	2.26888	2.15276	2.14176	8.21829	9.13542	9.29316	9.41399
Sector 1	2.41286	2.04596	2.21903	2.25198	8.4352	8.85722	8.72717	8.80193
Sector 2	2.19784	2.79665	2.28814	2.27546	8.70015	8.3938	8.94824	9.34835
Sector 3	2.16608	2.61122	2.15802	2.18627	10.1284	9.57484	9.61132	9.6551
Sector 4	2.01537	2.57255	2.22686	2.25348	8.92557	9.44247	9.14476	9.3292
Sector 5	2.06956	2.66318	2.42038	2.42122	9.47624	9.81359	9.99037	10.3113
Sector 6	2.25841	2.42244	2.29083	2.33922	11.4943	9.79248	11.2142	11.1528
Sector 7	2.79586	2.34265	2.45208	2.47559	11.7844	11.6089	12.5448	12.5788
Sector 8	2.64262	2.47602	2.57801	2.54309	10.0508	12.0831	12.4991	12.6981
Sector 9	2.27969	2.41338	2.34208	2.3257	11.241	11.9691	11.8146	11.9165
Sector 10	1.98771	2.07526	2.21118	2.23513	10.9893	10.3756	10.1515	10.2485
Sector 11	1.88262	2.02158	2.03392	2.07537	8.64952	10.1864	10.1237	10.1256

L-BFGS-B	Shape	Shape	Shape	Shape	Scale	Scale	Scale	Scale
	Anholt 2013-2014	Dudgeon 2019-2020	Dudgeon 2012-2022	Dudgeon 2002-2022	Anholt 2013-2014	Dudgeon 2019-2020	Dudgeon 2012-2022	Dudgeon 2002-2022
Sector 0	2.26949	2.30066	2.23116	2.18559	8.32611	9.3784	9.34265	9.41399
Sector 1	2.24203	1.79944	2.22361	2.26074	8.7216	9.07404	8.67463	8.80193
Sector 2	2.0573	2.85293	2.37606	2.3294	8.7098	8.82591	9.12724	9.34835
Sector 3	2.12964	3.02497	2.27291	2.22767	9.93498	10.7943	9.77552	9.6551
Sector 4	1.9831	2.76049	2.18368	2.21799	8.60506	10.2253	9.35001	9.3292
Sector 5	1.88007	2.59319	2.46843	2.44944	9.62261	10.2806	10.3105	10.3113
Sector 6	2.24343	2.5377	2.35075	2.44904	11.8112	10.112	11.4027	11.1528
Sector 7	3.14155	2.67872	2.57247	2.55557	12.3051	11.7496	12.8176	12.5788
Sector 8	2.84553	2.6305	2.64735	2.60664	10.2106	12.2679	12.6251	12.6981
Sector 9	2.29903	2.26523	2.34947	2.32831	11.3293	12.3041	12.0121	11.9165
Sector 10	1.91082	2.33533	2.25645	2.28942	11.081	9.71771	10.0621	10.2485
Sector 11	2.00601	2.18027	2.07809	2.08958	8.14514	9.45865	9.95996	10.1256

E Appendix - KS-stat and p-values for Dudgeon and Anholt

KS-Test	KS-stat (D)	KS-stat (D)	KS-stat (D)	KS-stat (D)
	Anholt 2013-2014	Dudgeon 2019-2020	Dudgeon 2012-2022	Dudgeon 2002-2022
Sector 0	0.05098820720219022	0.037473755545902376	0.024555962068481 54	0.019591915639261603
Sector 1	0.03259945831109279	0.05943973866029345	0.015142561349887007	0.016218440468560 69
Sector 2	0.02983631353022919 7	0.06722740850722075	0.029779642660945 57	0.025087136316336 3
Sector 3	0.04457668432906869 4	0.12226022449845153	0.029355224852798956	0.033520726937743 55
Sector 4	0.04975354475873661	0.09654528828945 83	0.019981929471609816	0.021184434114213002
Sector 5	0.03757478130073366	0.06950021996585554	0.036912795511800 93	0.026514961935952652
Sector 6	0.04552591106823722 4	0.05200546834419028 7	0.026576704301369436	0.030235717883060453
Sector 7	0.05561637261176982 6	0.06430032892646 17	0.033322604518183696	0.028274557744704387
Sector 8	0.03048334193242058 2	0.03885313876773355	0.019291294835384 22	0.017002167364063236
Sector 9	0.01677073377636 57	0.05638758003431199	0.021482721009913996	0.014439902392358372
Sector 10	0.03053843881107976	0.06936891149661395	0.019938432440636 2	0.016643228137682 71
Sector 11	0.03819405880332227	0.05985108612507406	0.017489072197385935	0.015288814485607 26

P-value	P-value	P-value	P-value	P-value
	Anholt 2013-2014	Dudgeon 2019-2020	Dudgeon 2012-2022	Dudgeon 2002-2022
Sector 0	2.735345186443032 6e-06	0.95391478668694 33	0.200205083752526 44	0.11596360759089153
Sector 1	0.00172803961903442 3	0.85865679275918 57	0.882960107034309 2	0.38869615765224 04
Sector 2	0.00130012966362380 5	0.48588442438924584	0.077138251372770 08	0.028273992961549 42
Sector 3	2.68067235690074 4e-07	0.02701709245474270 8	0.101855881249451 55	0.001133387783861 8498
Sector 4	2.73744097135801 8e-07	0.04574438015697268 6	0.499510437860589 8	0.083320036499843 32
Sector 5	4.68394263757611 5e-05	0.18951794553140 61	0.004775404521928 5095	0.003130667744533214
Sector 6	1.00949134558620 75e-10	0.39510773052696 89	0.036776669000257 11	6.233875665822058e-05
Sector 7	9.53447147001325 1e-18	0.07004386068064561	0.000359127844644 52803	1.390431430824223 5e-05
Sector 8	2.87298288167611 8e-05	0.41783367598144 37	0.062772074426306 5	0.010301229954054891
Sector 9	0.03479959282316 2584	0.30940346960932 94	0.107843367130210 25	0.13773288500277 28
Sector 10	0.00076812102612 1536	0.26746255568943933	0.376832578340917 3	0.17921838192802 23
Sector 11	0.00415303996892 3397	0.38620678151262 9	0.611197393556975 2	0.312453762794562 05

F Appendix - Wind sectors at Dudgeon with MLE method

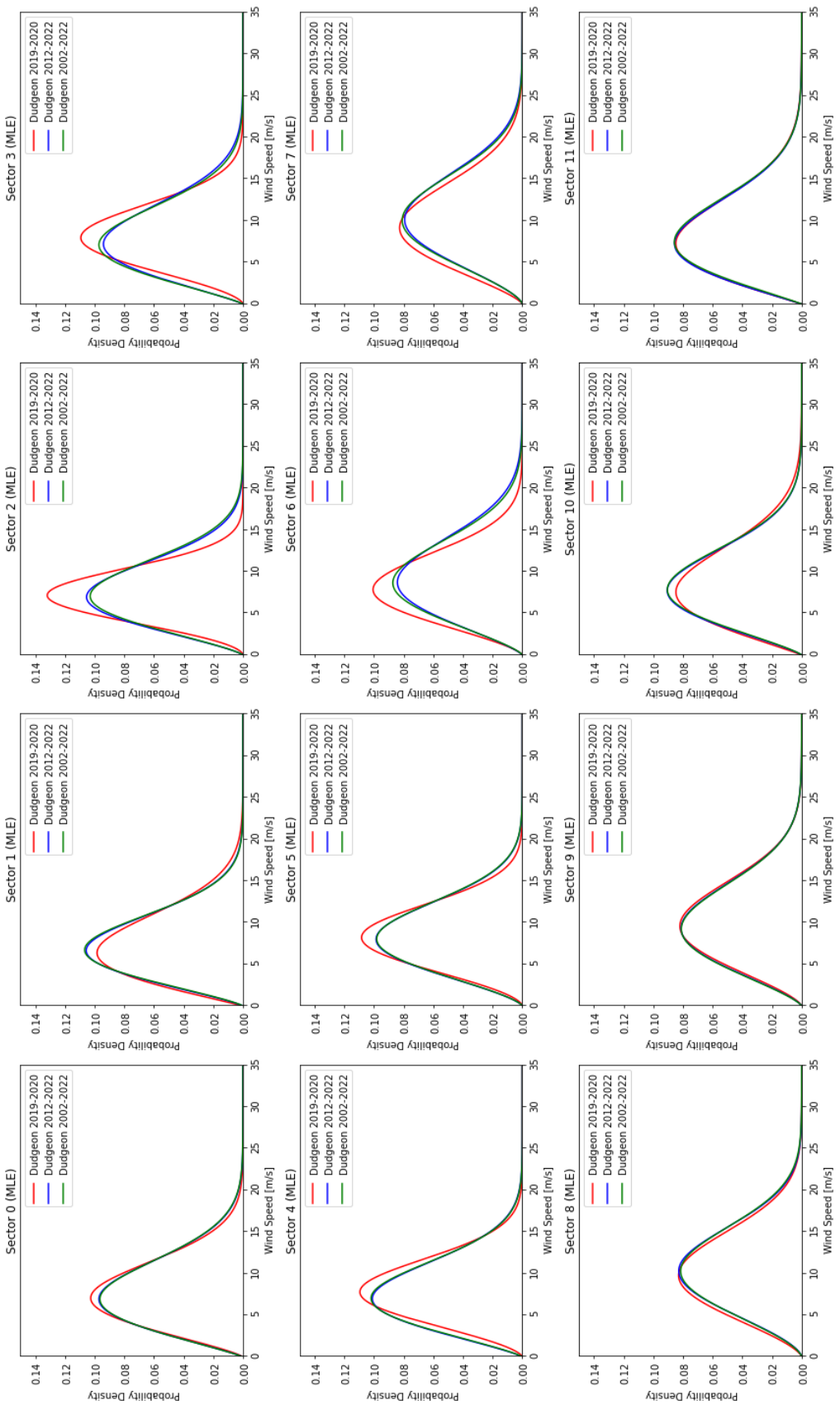

G Appendix - Wind sectors at Dudgeon with L-BFGS-B method

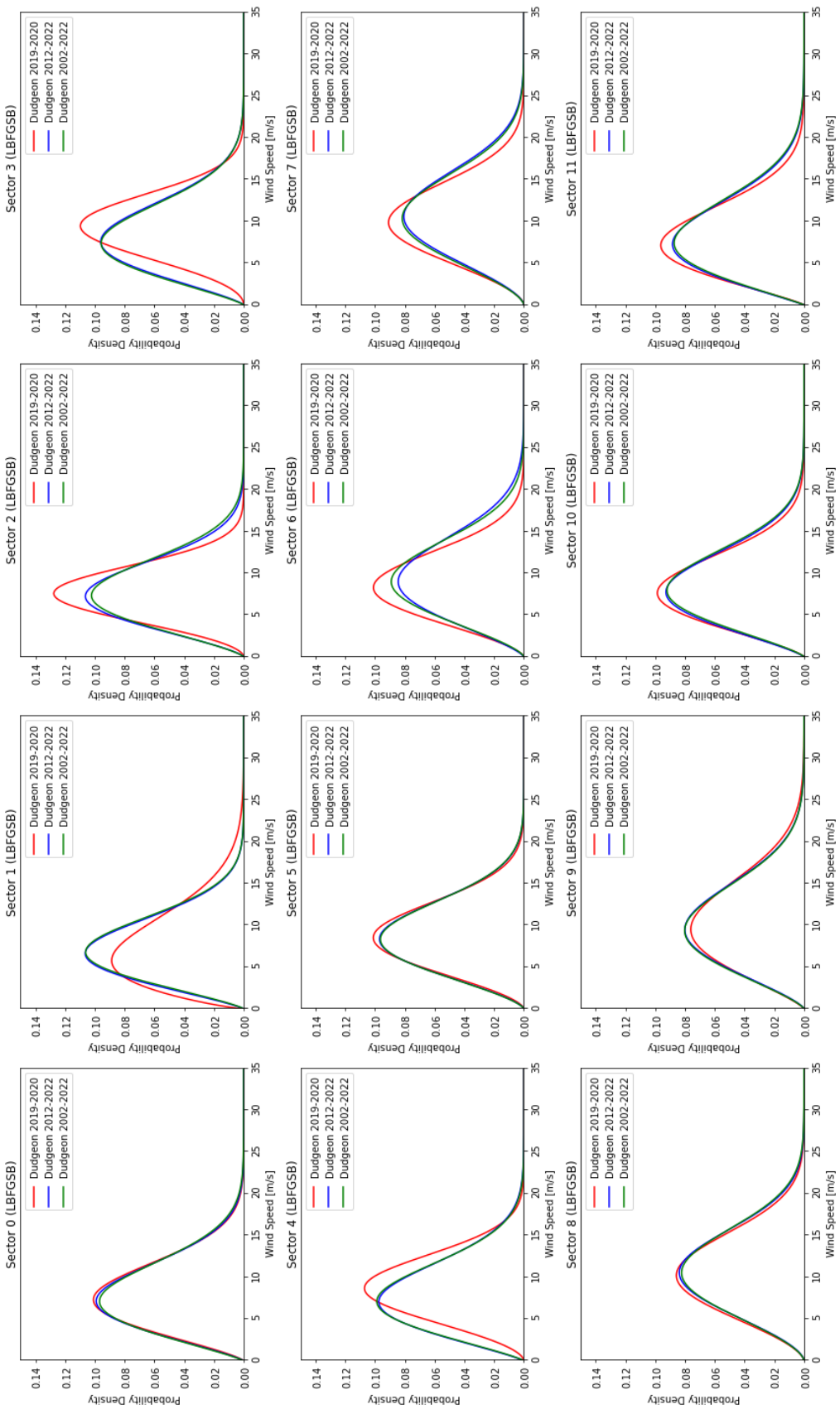

H Appendix - Wind sectors for Dudgeon and Anholt with MLE method

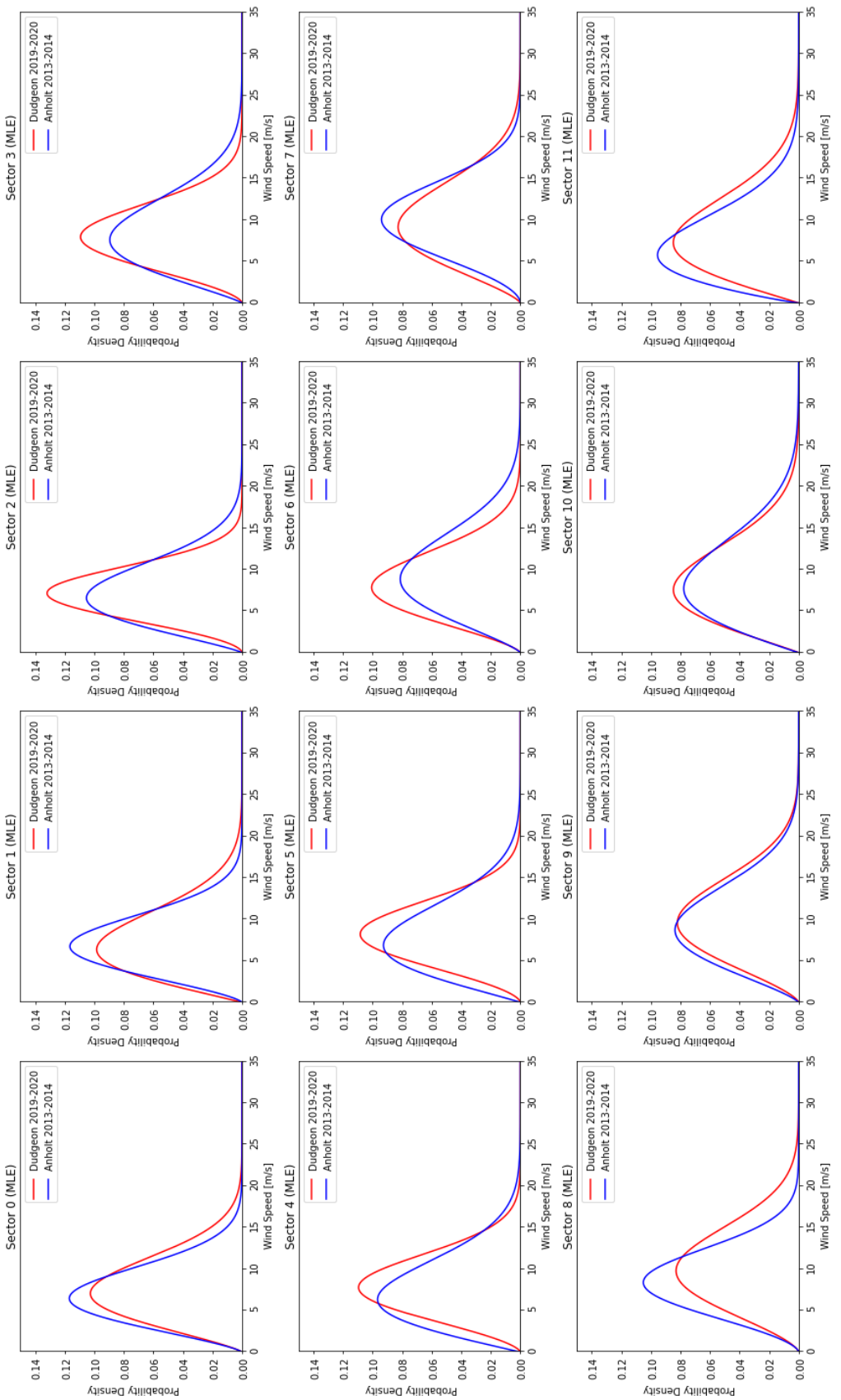

I Appendix - Wind sectors for Dudgeon and Anholt with L-BFGS-B method

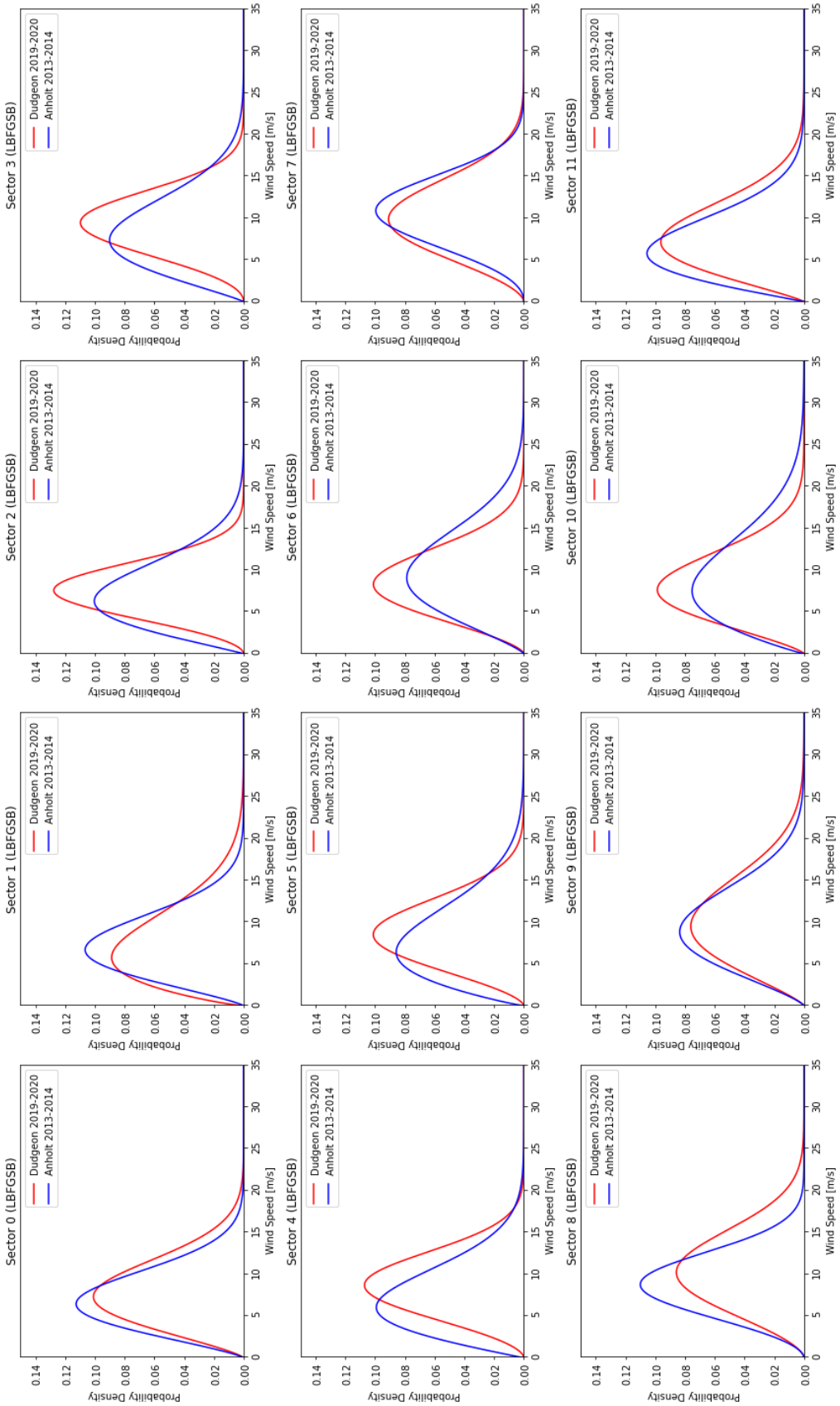

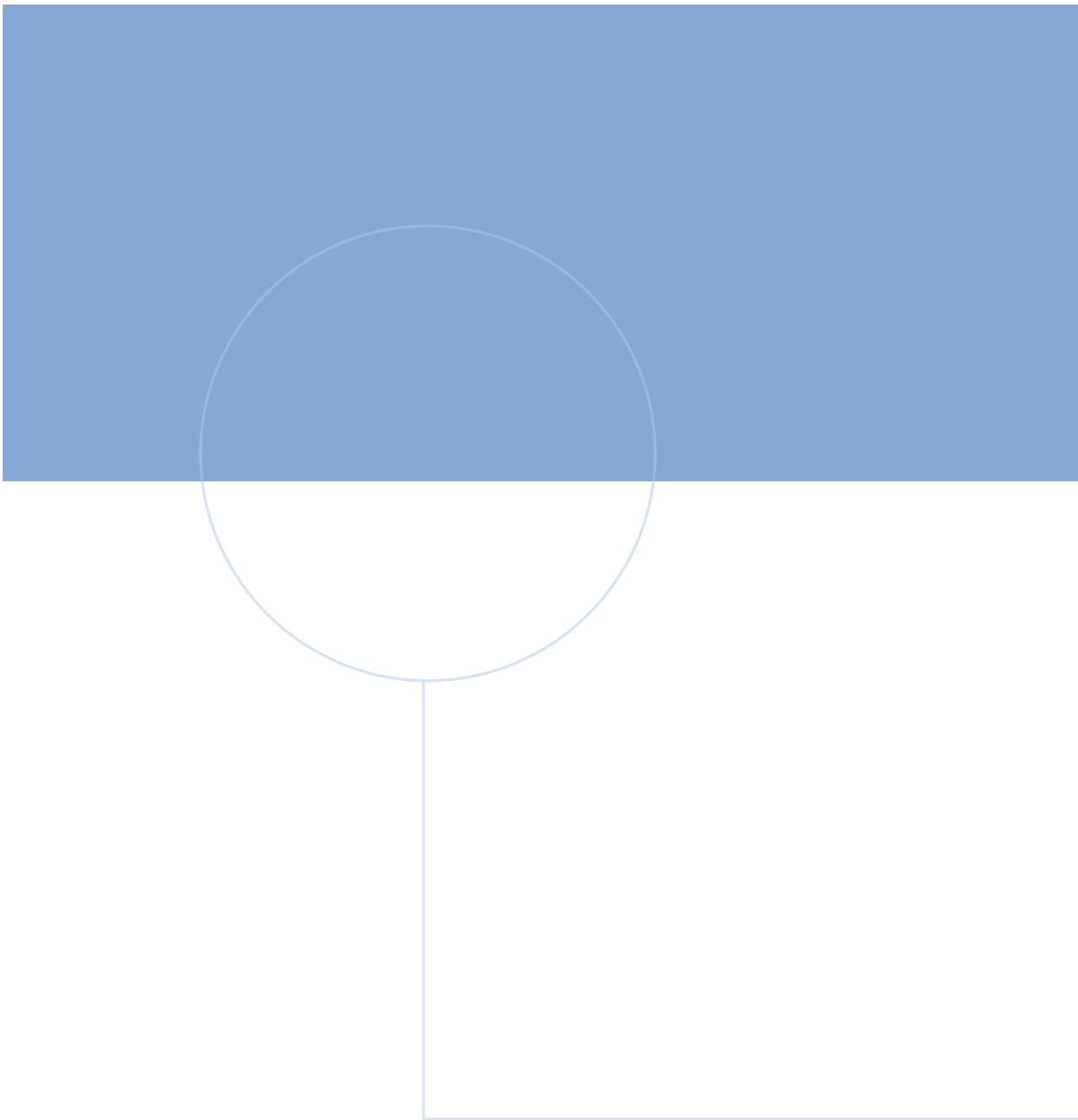

NTNU

Norwegian University of
Science and Technology